A THESIS SUBMITTED TO
THE GRADUATE SCHOOL OF NATURAL AND APPLIED SCIENCES
OF ÇANKIRI KARATEKİN UNIVERSITY

GROWING DOPED (Cu-Sn) AND UNDOPED ZnO SEMICONDUCTOR THIN FILMS BY SILAR METHOD; STRUCTURAL AND ELECTRICAL CHARACTERIZATION

IN PARTIAL FULFILLMENT OF THE REQUIREMENTS
FOR
THE DEGREE OF MASTER OF SCIENCE
IN
PHYSICS

BY

FIRAS MUAYAD HABEEB HABEEB

ÇANKIRI

2023

GROWING DOPED (Cu-Sn) AND UNDOPED ZnO SEMICONDUCTOR THIN FILMS BY SILAR METHOD; STRUCTURAL AND ELECTRICAL CHARACTERIZATION

By Firas Muayad Habeeb HABEEB

February 2023

We certify that we have read this thesis and that in our opinion it is fully adequate, in scope and in quality, as a thesis for the degree of Master of Science

Advisor : Asst. Prof. Dr. İlker KARA

Examining Committee Members:

Chairman : Prof. Dr. Özcan YALÇINKAYA
Department of Chemistry
Gazi University

Member : Assoc. Prof. Dr. Olcay GENÇYILMAZ
Department of Material and Material Processing Technologies
Çankırı Karatekin University

Member : Asst. Prof. Dr. İlker KARA
Department of Medical Services and Techniques
Çankırı Karatekin University

Approved for the Graduate School of Natural and Applied Sciences

Prof. Dr. İbrahim ÇİFTÇİ
Director of Graduate School

I hereby declare that all information in this document has been obtained and presented in accordance with academic rules and ethical conduct. I also declare that, as required by these rules and conduct, I have fully cited and referenced all material and results that are not original to this work.

Firas Muayad Habeeb HABEEB

ABSTRACT

GROWING DOPED (Cu-Sn) AND UNDOPED ZnO SEMICONDUCTOR THIN FILMS BY SILAR METHOD; STRUCTURAL AND ELECTRICAL CHARACTERIZATION

Firas Muayad Habeeb HABEEB

Master of Science in Physics

Advisor: Asst. Prof. Dr. İlker KARA

February 2023

In this thesis study, structural and electrical characterization of undoped and Sn-Cu doped ZnO thin films grown on ITO substrate by using the SILAR method were performed. The grown thin films were obtained by performing 40 times SILAR cycle and annealed at 300 °C. Doped ZnO thin films were obtained by keeping the copper (Cu) doping ratio constant and changing the tin (Sn) doping ratio from 1 % to 3 %. The structural, surface morphological and electrical properties of the produced undoped and Sn-Cu doped thin films were investigated. From SEM analyzes, it was observed that the films produced without additives and with different concentrations of Sn-Cu grew spherically (from 64 nm to 177 nm) depending on the concentration on the ITO substrate, and their morphological properties changed depending on the doping concentration. From electrical analyzes, doping processes at different rates (I-V) give positive results and it is thought that produced thin films can be used as a transparent carrier film (TCO) because they do not have high resistance.

2023, 73 pages

Keywords: SILAR method, Zinc oxide, Thin films

ÖZET

SILAR YÖNTEMİYLE (Cu-Sn) KATKILI VE KATKISIZ ZnO YARİİLETKEN İNCE FİLMLERİN BÜYÜTÜLMESİ; YAPISAL VE ELEKTRİKSEL KARAKTERİZASYONU

Firas Muayad Habeeb HABEEB

Fizik, Yüksek Lisans

Tez Danışmanı: Dr. Öğr. Üyesi İlker KARA

Şubat 2023

Bu tez çalışmasında, SILAR yöntemi kullanılarak ITO alltaş üzerine büyütülen, katkısız ve Sn-Cu katkılı ZnO ince filmlerin yapısal ve elektriksek karekterizasyonu yapılmıştır. Büyütülen ince filmler 40 kat SILAR döngüsü yapılarak elde edildikten sonra 300 °C'de tavlanmışlardır. Katkılı ZnO ince filmlerde bakır (Cu) katkı oranı sabit tutularak, kalay (Sn) katkılama oranı % 1'den % 3'e değiştirilerek elde edilmiştir. Üretilen katkısız ve Sn-Cu katkılı ince filmlerin yapısal, yüzeysel morfolojik ve elektriksel özellikleri incelenmiştir. SEM analizlerinden katkısız ve farklı Sn-Cu katkı konsantrasyonuna bağlı olarak üretilerin filmlerin ITO alltaş üzerine küremsi (64 nm'den 177 nm'ye) birşekilde büyüdüğü ve katkı konsantrasyonuna bağlı olarak morfolojik özelliklerinin değiştiği gözlendi. Elektriksel analizlerinden (I-V) farklı katkılama işleminin olumlu sonuçlar verdiği ve üretilen ince filmlere yüksek dirençe sahip olmamasından dolayı şeffaf taşıyıcı film (TCO) olarak kullanılabileceği düşünülmektedir.

2023, 73 sayfa

Anahtar Kelimeler: SILAR metodu, Çinko oksit, İnce film

PREFACE AND ACKNOWLEDGEMENTS

I would like to thank my thesis advisor, my dear teacher Asst. Prof. Dr. Ilker KARA, who contributed to the preparation of my master's thesis. I would also like to thank my family for their financial and moral support.

Firas Muayad Habeeb HABEEB
Çankırı-2023

CONTENTS

LIST OF SYMBOLS

A	Absorbance value
α	Absorption coefficient
Å	Angstrom value
β	Half peak width
°C	Centigrade degree
Cs	Crystal size
d_{hkl}	Interplaner distance
d_{XRD}	Experimental distance
d_{CARD}	Standard distance
E_g	Energy gap
E_{ph}	Phonon energy
eV	Electron volt
h	Planck's constant
I	Transmittance intensity
I_A	Absorbed intensity
I_R	Reflected intensity
I_o	Standard (Incidence) intensity
K	Shape factor
k_o	Extinction coefficient
k_B	Boltzman constant
λ	Wavelength
M	Molar value
$M_{(hkl)}$	Miller indices
nm	Nanometer value
n_o	Refractive index
N	Complex refractive index
R	Reflectance
δ	Dislocation density
ν	Frequency value
T	Transmittance value
TCO	Transparent conductive oxides
θ	Bragg angle

LIST OF ABBREVIATIONS

EDS	Energy dispersive X-ray spectroscopy
FESEM	Field emission scanning electron microscope
UV-VIS	Ultraviolet-visible
XRD	X-ray diffraction

LIST OF FIGURES

LIST OF TABLES

1. INTRODUCTION

1.1 Overview of Translucent Transfer Oxides (TCO)

The study of semiconductor materials, notably transparent carrier oxides, which are among the most important Basic materials used in the manufacturing of thin films, began at the turn of the nineteenth century. In the field of carrier oxides, there has been a lot of research and discoveries. Transparency in the long run (Burgelman 2006).

- After the discovery of indium oxide spotted with tin in 1954, the first usage transparent carrier oxides was made (In_2O_3:Sn) By Scientist (G.Rupprecht).
- Binary compounds like (SnO-In_2O_2-ZnO) first arose in the 1960s and were proved to be good transparent conductive oxides.
- Within a year (1980), various ternary compounds, such as (Cd_2SnO_4), as well as compounds containing multiple compounds, arose.

The translucent conductive oxides were predominantly (n-type) semiconductors, with a small amount of p-type. These transporting oxides were numerous, as discovered by the researcher (H. Sato) with his partners in nickel oxide in 1993. Its transparency and a wide range of qualities make it a fascinating material that can be used for research and applications. It sped up the development of various sectors, including electrical, optical, and structural properties. The notion of transparent carrier oxides and its most prominent applications will be presented on this foundation, and we will discuss in more detail in the following sections. The latter on zinc oxide, which will be the focus of our investigation in the next chapters.

1.2 Definition of Transparent Conductive Oxides

Materials are divided into three kinds based on the principle of energy bands conductors, insulators, and semiconductors. The transport band (BC) and the valence band (BV), which allow electrons to freely migrate, have an overlap. Whereas the insulator has a

large forbidden band with a value of about (5 eV) called the energy separator symbolized by the symbol (E_g) in which the electrons can only move when they receive a sufficient energy equal to or greater than their energy separator (Abdallah *et al.* 2018).

As for semiconductors, the value of the energy separator is much lower than that of insulators, and it is characterized by its great influence on temperature, as it is an insulator at absolute zero temperature so that the transport package (BC) is empty, meaning that there are no free electrons and it is a conductor at high temperatures. At normal room temperature, the resulting current is weak and cannot be benefited from, because the number of electrons gaining energy and transferring to the conduction band is few, and thus these materials are neither good conductors nor insulators. The image below also shows how natural materials are classified into three categories based on their electrical conductivity: insulator, semiconductor, and conductor (Figure 1.1) (Ayouchi *et al.* 2003, Abdallah *et al.* 2018).

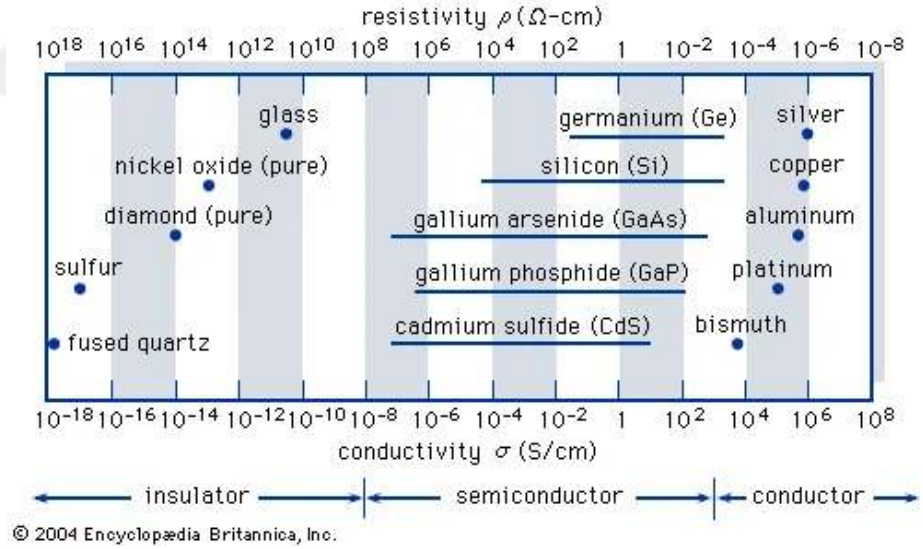

Figure 1.1 The conductivity range of some conductive materials, semiconductors and insulators (Saha *et al.* 2007).

Transparent conductive oxides are among the most important compound semiconductors made of metal combined with oxygen (Saha *et al.* 2007). That is, they are oxide compounds like ZnO and SnO, which we will examine in more detail later. The oxides have a considerable energy separation due to oxygen gaps generated by the uneven

molecule (Mabayoje *et al.* 2016), the transport bundle is full of free electrons, and it is characterized by strong conductivity and optical transmittance in our investigation of ZnO. Its Fermi level is relatively close to the transport band (BC), implying that there is a large energy gap between them ($3 \leq E_g \leq 4.6$) (Turgut *et al.* 2015).

There are two types of metal oxides: simple metal oxides with only one metal and complex metal oxides with many metals. Some of these oxides are shown in Table 1.1.

Table 1.1 Simple and compound oxides

Simple Oxides	**ZnO**	**CuO**	**NiO**
Complex Oxides	Cnd_2SnO_4	$BaTiO_3$	$CdInO_4$

1.3 The Most Important Characteristics of Transparent Carrier Oxides

- Its electrical conductivity rises with temperature, which is one of the properties that distinguishes it from the other Carrier materials, and it becomes semi-insulating at low temperatures (Chen *et al*. 2007).
- The semiconductor has a high sensitivity, which can result in an increase in conductivity when it contains impurities or flaws, since it can result in one type of charge carrier diminishing or disappearing (Chen *et al.* 2007).
- Electrical conductivity and high transparency at visible wavelengths (400 - 800 nm).

1.4 Criteria for the Selection of Transparent Carrier Oxides (TCO)

In order to find out the best transparent carrier oxides and distinguish between them, the scientist (G. Haache) proposed a parameter called quality factor in the year (1976) (Bernardi *et al.* 2002, Yadav *et al*. 2009). This number links the transparent carrier oxide's optical and electrical properties. The square resistance of the transparent carrier oxide layer is defined as the ratio between the average transmittance (T) in the visible field and the surface resistance, and its unit is (Ω^{-1}) (Mazhir and Harb 2015).
It is given by the relationship Equation (1.1):

$$\mathbf{F}_{TC} = \frac{\mathbf{T^{10}}}{\mathbf{R_S}} \quad (1.1)$$

Note that:

F_{TC}: quality factor (Ω^{-1})

T: permeability.

R_S: surface resistance (Ω)

As shown in the Table 1.2, the scientist (G. R Gordon) compared the clear carrier oxides based on the quality coefficient of each component.

Table 1.2 The quality parameters of some transparent carrier oxides

Materials	**Quality factor (Ω^{-1})**	**Referance**
ZnO by doped F	7	11
Cnd_2SnO_4	7	
ZnO by doped Al	5	
In_2O_3	4	
SnO_2 by doped F	3	
ZnO by doped Ga	3	
ZnO by doped B	2	
SnO_2 by doped Sb	0.4	
ZnO by doped in In	0.2	

Aside from appropriate electrical and optical qualities, there are other significant factors to consider, such as the material used. Different deposition processes, production costs or material toxicity, heat and chemical resilience of the films are all factors to consider (Ayouchi *et al.* 2003).

1.5 Electrical and Optical Properties of Transparent Carrier Oxides (TCO)

Because of their great transparency, superior electrical conductivity, and deposition process, transparent carrier oxides have crucial electrical and optical features, which has prompted researchers to examine them in order to develop and benefit from them. These materials' electrical and optical properties are best within the boundaries of the amounts listed in the Table 1.3 below (Turgut *et al.* 2015).

Table 1.3 The properties of transparent carrier oxides.

Properties (TCO)	**Amount**
Energy splitter Eg (eV)	(3 - 4.2)
Resistivity ρ (Ω.Cm)	Less than ($1.0 \text{ -}10^{-4}$)
Surface resistance R_S (Ω)	From 10 to some thousands
Kinetic μ ($Cm^2/V.s$)	Up to 50
Density of charge carriers (cm^{-3})	More than ($1.0 \text{ - } 10^{20}$)
Permeability T	More than (90 %)
Absorption coefficient α (cm^{-1})	Less than ($1.0 \text{ - } 10^4$)

1.5.1 Electrical properties

Transparent carrier oxides (TCO) have been studied electrically since 1970, and these oxides are classed as semiconductors with a reasonably large energy interval based on their electrical properties, we mention these characteristics:

1.5.2 Energy gap (E_g)

The energy gap in transparent conductive oxides, often known as the energy gap, is large (3 - 4.2) eV (Turgut *et al.* 2015). The breadth of the separator varies depending on the sedimentation technique utilized and the conditions of the experiment. It also relies on the sort of substance that has been employed, Table 1.4 shows the energy interval for some oxides.

Table 1.4 The energy interval for some transparent conductive oxides

Transparent carrier oxides	Energy gap (Eg)	References
SnO_2	(3.6 - 4.3) eV	(12 - 13)
ZnO	(3.2 - 3.3) eV	(14 - 15)
TiO_2	(3 -3.2) eV	(7)
NiO	(3.6 - 4) eV	(16)

1.5.3 Electrical conductivity and resistance

The electrical conductivity is indicated by the symbol (σ) and its unit is ($\Omega.cm^{-1}$). It is a measure of a medium's ability to transfer an electric charge through it. It is expressed by the relationship Equation (1.2) (Turgut *et al.* 2015).

$$\sigma = \frac{1}{\rho} q.n.\mu \qquad (1.2)$$

Note that:

q: the type of charge (C)

n: density of charge carriers (cm^{-3})

μ: kinetics of charges ($cm^2/V.s$)

The symbol (ρ) represents electrical resistance: it expresses the resistance of a matter to the flow of electric current through it, and its unit is centimeters. Low-resistance materials are good conductors, while high-resistance materials are good insulators (Chen *et al.* 2007).

1.5.4 Surface resistance

The surface resistance is one of the most important electrical properties of transparent conductive oxides, as it is expressed as the ratio of the electrical resistance (ρ) to the thickness of the thin film (d), and is symbolized by the symbol (R_S), Its unit (**Ω**) It is expressed by the relationship Equation (1.3) (Richard 2013).

$$R_S = \frac{\rho}{d} \tag{1.3}$$

1.5.5 Electrical kinematics

The electrical mobility of a material is represented by (μ), which basically expresses the mobility of charge carriers in the crystal lattice of the material and is one of the variables that determine electrical conductivity, and its unity ($cm^2.V^{-1}.s^{-1}$) It is expressed by the relationship Equation (1.4) (Mazhir and Harb, 2015).

$$\mu = \left(\frac{q.\tau}{m^*} = \frac{q.I}{m^*.v}\right) \tag{1.4}$$

Note that:

q: Electron speed

τ: Relaxation time between collisions

m^*: Effective mass of the electron

I: Average free path

v: Thermal velocity of the electron

1.5.6 Dielectric constant

The dielectric constant express a material's ability to polarize, as it responds to different frequencies with a complex behavior (imaginary number), and at optical frequencies represented by light waves, electronic polarization is dominant only over the other types of polarization, and the degree of polarization of the material is dependent not only on the electric field, but also on the molecular properties of the material that make it up. The interaction of light with the medium's charges is frequently explained, and the polarization of the charges that results is referred to as the complex dielectric constant of the medium (Kumar *et al.* 2006). It is expressed by the relationship, Equation (1.5).

$$\varepsilon = \varepsilon_1 - i\varepsilon_2 \qquad (1.5)$$

Note that:

ε: Complex dielectric constant.

ε_1: The real part of the dielectric constant.

$i\varepsilon_2$: Composite part of the dielectric constant.

1.5.7 Optical properties

The ubiquitous use of transparent carrier oxides in various commercial and laboratory domains underscores the relevance of researching their optical characteristics. These characteristics are reflected by the following basic phenomena:

1.5.8 Permeability (T)

It is expressed by the symbol T, and it is discribed as the ratio between the intensity of radiation passing through the material (I_T) to the initial intensity of the radiation falling

on the material (Mazhir and Harb 2015) and is given by the relationship Equation (1.6) (Al-Jawad *et al*. 2016).

$$T\ (\%) = \left(\frac{I_T}{I_0}\right) . 100 \qquad (1.6)$$

The transmittance spectrum is mostly determined by the number of energy levels, which is determined by the material's chemical and crystalline composition, as well as thickness and grafting variables.

1.5.9 Reflectivity (R)

It is symbolized by the letter R, and it is discribed as the ratio of the intensity of the light reflected on the material's surface IR to the intensity of the light falling on it I_o, as provided by the relationship Equation (1.7) (Van Hieu *et al.* 2010).

$$R\ (\%) = \left(\frac{I_R}{I_0}\right). 100 \qquad (1.7)$$

1.5.10 Absorbance (A)

It is symbolized by the letter A, and it is discribed as the ratio of the intensity of the light absorbed by a substance (I_A) to the intensity of the incoming light (I_o), as provided by the relationship Equation (1.8) (Van Hieu *et al*. 2010).

$$A\ (\%) = \left(\frac{I_A}{I_0}\right). 100 \qquad (1.8)$$

And we can write the following Equation (1.9) and Equation (1.10) because the total flow is conserved:

$$I_0 = I_R + I_T + I_A \qquad (1.9)$$

$$T + R + A = 1 \qquad (1.10)$$

1.5.11 Absorbance coefficient (α)

It is symbolized by the symbol, and we use the (Ber-Lumber) connection to determine it, which links the light flux transmitted and the absorption coefficient, and is provided by the relationship Equation (1.11) (Pal and Chauhan 2009).

$$\alpha = \frac{\mathbf{1}}{\mathbf{d}} \ln \left(\frac{100}{T(\%)}\right) \quad (1.11)$$

α: Absorbance coefficient (cm^{-1})

T: Permeability

d: Thickness (cm)

1.5.12 Damping coefficient (K)

The amount of energy absorbed by the electrons of the matter from the energy of photons of radiation falling on it is expressed by this coefficient, which is related to the absorption coefficient (α) by the following relationship Equation (1.12) (Bakr *et al.* 2018).

$$K = \frac{\alpha.\lambda}{4\pi} \quad (1.12)$$

λ: The wavelength of the incident rays.

1.5.13 Refractive index (n)

The real element of the complex refractive index is the ratio of light's speed in free space (c) to its speed in the medium (v) Equation (1.13) (Khoudro and Najeeb 2020).

$$n = \frac{C}{V} = \left[\left(\frac{1+R}{1-R}\right)^2 - (K^2+1)\right]^{1/2} + \frac{1+R}{1-R} \quad (1.13)$$

R: Reflectivity

K: Damping coefficient

The cooling index (K), refractive index (n), and energy interval (E_g) can be calculated by measuring the transmittance, reflectance, and thickness of the transparent conductive oxides (Srivastava *et al.* 2008).

1.6 Translucent Oxides Carrier Applications

Since many applications require this combination of optical transparency and electrical conductivity, it is widely used (Tabet 2013).

- Screens that are flat
- Cavity for lasers
- Electro-optical mirrors are the third type of mirror
- Anti-electromagnetic shielding
- A gas detector
- Windows that reflect heat (buildings and ovens)
- Touch screen control
- A diode made of organic materials

Sun cells have a front contact through which light must flow in order for it to reach the solar cell (Figure 1.2).

Figure 1.2 The applications of transparent carrier oxides (Tabet 2013)

1.7 Zinc Oxide (ZnO)

1.7.1 Zinc oxide concept (ZnO)

It's a large-gap semiconductor with excellent transparency at visible and sub-visible wavelengths. It is an inorganic compound of formula that is red and comprises of group (II-VI) and is generally n-type. ZnO is a non-polluting, non-toxic, and readily available mineral. It appears as a white powder that dissolves in water or alcohol, and laboratories rely on zinc oxide preparation. Chemically, by burning zinc in the air or shattering its carbonates or nitrates with heat, Table 1.5 presents some of its characteristics (Kang *et al.* 2018).

Table 1.5 Some physical and chemical properties of zinc oxide

Crystal structure	Molar mass g/mol	Density g/cm^3	Melting point (C^o)	Boiling point (C^o)	The shape	The color
Hexa	81.37	5.67	110/1970	2360	Solid	White

1.7.2 Structural properties of zinc oxide

In general, the second-sixth group semiconductors (II-VI) crystallize in the periodic table in the structure (CFC) or in the structure (HC) wurtzite, and zinc oxide (ZnO) can be found in nature as a powder (poudre) or as a solid (HC) wurtzite (cristal mountainous) (Goriunova and Anderson 1965). The crystal structure of zinc oxide can take three different forms dependently on the preparation conditions:

a- Rock salt's structure: is unstable and appears under high pressures.
b- Cubic structure: is unstable and emerges when pressures are really high.
c- Wurtzite Hexagonal: Under normal conditions, it is stable.

As shown in the Figure 1.3 (Ynineb 2015).

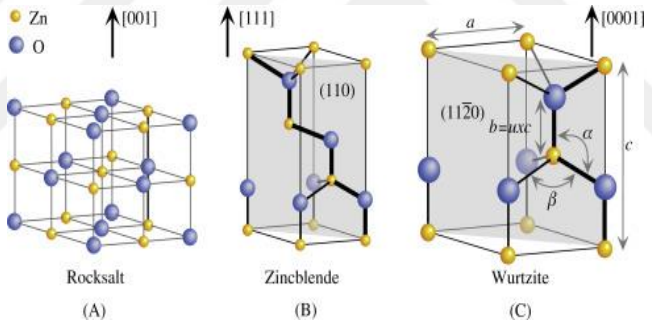

Figure 1.3 The three possible structures of zinc oxide (Reddy *et al.* 2002)

The hexagonal structure is the most stable and prevalent in nature among these sorts, own this structure grid constants (a = 3.249 A^{o}) and (c = 5.207 A^{0}), as well as a value (c/a) that is quite close to the ideal cell value hexagram, which is equal to 1.633 A^{o} (He *et al*. 2013).

In the hexagonal configuration, the zinc and oxygen atoms are arranged as follows (Perna and Capozzi 2002).

Zn : (0,0,3/8), (2/3,1/3,7/8)

O : (0,0,0), (2/3,1/3,1/2)

So that each zinc atom (Zn) has four oxygen atoms (O) surrounding it, and vice versa. In the hexagonal structure, this results in a (4:4) coordinate distribution of (Zn) and (O) atoms (Wurtzite) (Figure 1.4) (Zhang *et al.* 2013).

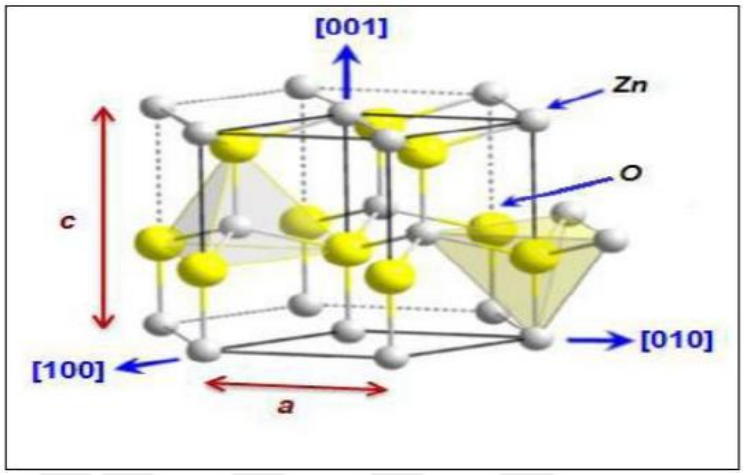

Figure 1.4 The agglutinating crystal structure of zinc oxide (Ynineb 2015)

1.7.3 Electrical properties of zinc oxide

1.7.4 Zinc oxide absorption edge (Energy gap)

When the energy of the absorbed radiation is almost equal to the energy gap, fast absorption occurs. It's known as the basic absorption edge, and it's a term that applies to all semiconductor materials The energy gap for zinc oxide varies between 2.3 eV and 3.3 eV, because an absorption edge may not emerge at the energy gap value in some materials, there will be two types of energy band transitions in a semiconductor (Subramanyam *et al*. 2000):

1) Transferts directs: Permitted direct transfer occurs when an electron moves from the top of the valence band to the bottom of the conduction band at the same point in space (K-Space), and forbidden direct transmission occurs when an electron moves from neighboring regions to the permitted direct transition regions with the condition that the value of the vector K remains unchanged, Figure 1.5 also demonstrates that ZnO has a direct energy gap and that its valence band is divided into three sub-bands.

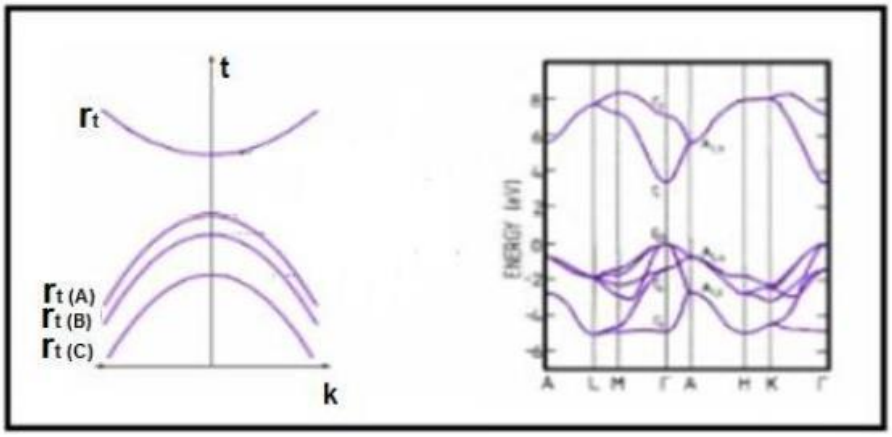

Figure 1.5 The direct energy gap of ZnO(Subramanyam *et al.* 2000)

2) Indirect transfers: When the energies of the top of the valence band and the bottom of the conduction band do not match in the vector space (k), the transition between the valence band and any point in the conduction band is not perpendicular, and the vector value is $\Delta K \neq 0$ (Figure 1.6).

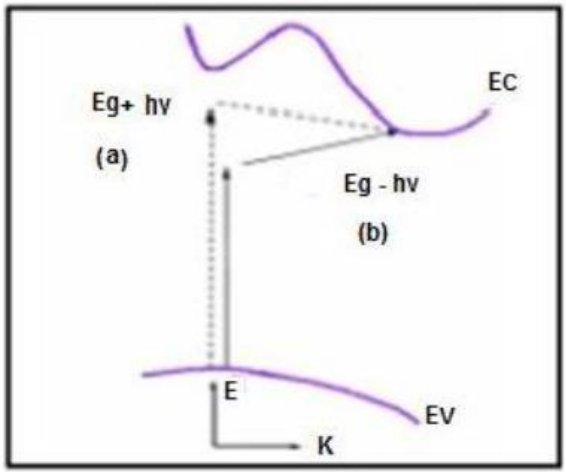

Figure 1.6 Electronic transmissions a) direct, b) indirect

1.7.5 Optical properties of zinc oxide

Zinc oxide is a transparent material with a refractive index of 0.2 in its solid form, but its refractive index varies between 1.9 and 2.2 in thin layers, therefore the refractive index and absorption change depending on the conditions of manufacturing (Al-Ani 2008). It

also has a high visible transmittance and strong infrared reflectance since its absorption coefficient in the visible band is within a certain range ($5x10^3$ cm^{-1}) (Mosiori 2015).

Aside from its transparency, zinc oxide has the property of illumination due to the action of beam energy in the top photodiode of the zinc oxide energy separator, ZnO, where photons are emitted from this zinc oxide. Photons have a wavelength of (550 nm), which is similar to green light (Moustaghfir 2004).

2. LITERATURE REVIEW

2.1 Thin Film Deposition Methods

One of the key areas of study in solid material physics is the study of materials in the form of thin films. The study of semiconductor physics has benefited greatly by thin films of both grafted and ungrafted metal oxides, In order to use these materials in a variety of applications, their physical and chemical properties have been investigated. Because it has replaced other materials of large sizes in achieving the same aims in contemporary semiconductor technology, electrical circuits, and many industrial uses, experimental work to manufacture these nano-thin layers has revolutionized the field of applications (Hussein *et al.* 2017).

When deposited under the right circumstances, thin films of impure metal oxides, such as tin oxide, indium oxide, cadmium oxide, and zinc oxide, etc., are optically transparent and electrically conductive (Pandya and Raval 2017).

Studies have shown that preparation methods have a significant impact on the quality and characteristics of thin films that are produced, so the researchers placed a strong emphasis on the diversification of preparation techniques (Biswal *et al.* 2014).

The broad principles of thin film deposition, as well as the mechanisms underlying their growth, are covered in this chapter. We'll also concentrate on the many physical and chemical processes and methodologies applied to thin film deposition. A brief discussion of some of the thin-film sample techniques and tools used to ascertain the various properties is also covered in this chapter's last section.

2.2 Thin Film Concept

Thin films, whose thickness does not exceed one micron, are arrangements of material constituents in two dimensions, with a very small third dimension (Biswal *et al*. 2014). Glass, silicon, aluminum, or quartz serves as the substrate for the deposition (Rahal 2013). Additionally, these films' thickness appears to be significant in modifying their physical characteristics. However, in the case of thin films, the influence of the surfaces on the characteristics is predominate. In the solid state of the material, we disregard the role of boundaries (surfaces) in the properties. The properties of the thin layer revert to those of the solid material once its thickness crosses a particular threshold since surfaces' effects on these layers are no longer taken into account (Wang *et al.* 2009).

The second benefit of thin films is the method of production, so we must consider the significance of substrate installation because it affects the structural, optical, and electrical properties of the thin film. For instance, according to research by Yusta and others on the influence and composition of the substrate on the characteristics of the precipitated thin films, we find that a slice of undoped SnO_2 precipitates as a thin film. Thin films that may impart volume properties on thin surfaces can thereby enable the economical use of resources in exchange for maintaining the physical properties afforded by volume, even if they may be the same thickness and made of the same materials (Hafdallah 2007).

2.3 Thin Film Deposition Principle

The choice of the appropriate method for deposition of thin films is one of the important factors, as it is directly related to the physical properties of those films. Over time, scientists have discovered and developed multiple methods for preparing thin films. The appropriate method for preparing the thin films is chosen according to the circumstances, the type of layer, the requirements of the layer, the cost of preparation and the available means. In order to deposit a thin film on the surface of a solid substrate, the particles of the material constituting the film must pass through a carrier medium so that this medium is in direct contact with the substrate (Choi *et al.* 1998), and once the particles reach the

surface of the substrate, part of them binds to the surface through (Van der Waals forces) or it reacts with it chemically as these particles are either ions or molecules and may be atoms. As for the transport medium, it may be liquid, gaseous, or vacuum.

- The state of the transport medium is liquid: This method is considered relatively easy, including the (sol-gel) method.
- The state of the transport medium is gaseous or vacuum: This medium is considered the most used in various methods of deposition, for example, chemical deposition of vapors. The gaseous medium differs from the vacuum medium in the value of the free median path, which is called (the path between the two collisions) (Kim *et al.* 2008).

It should be noted that there is no reference method for thin film deposition, as various methods can be used. In addition, substrate preparation is an important step to obtain good thin films (Yi *et al.* 1988).

2.4 Thin-Film Growth Mechanisms

The different deposition methods used include growth in three basic stages, production of ionic, molecular and atomic species. Where these ions, molecules or atoms are transferred to the substrate (Kamal *et al*. 2004). Then these produced elements are condensed on the substrate either directly or by chemical reaction to form solid films on this substrate and this stage in turn is divided into three stages: nucleation, coalescence and growth (Benhaoua *et al.* 2014).

2.4.1 Nucleation Stage

At this stage, small groupings of the sedimentary material appear on the upper surface of the glass. This stage is accompanied by changes in the state of the material, and these changes are represented in the turning point that develops the state of the material into a chemical or physical structure at these points (types) of ions or atoms coming to substrate

(Gâlcă *et al.* 2010). These aggregates (les agrégats or clusters) interact with the substrate and form unstable assemblies on the surface of the substrate and are points for the assembly of other atoms to start the growth of thin layers or films (Figure 2.1).

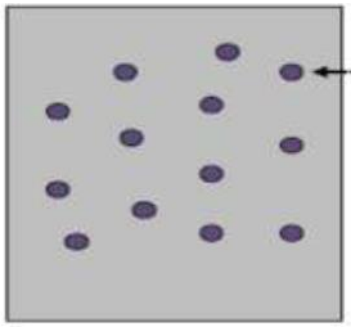

Figure 2.1 Nucleation stage

2.4.2 Adhesion stage

When the size of the gatherings formed in the previous stage increases, they coalesce among themselves and gradually approach each other, forming islands on the surface of the substrate (Figure 2.2) (Gâlcă *et al*. 2010).

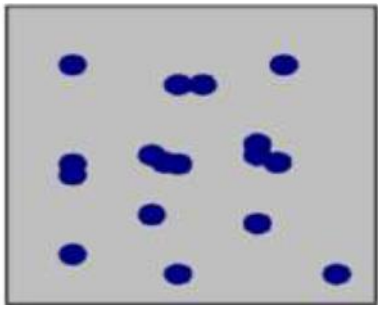

Figure 2.2 Adhesion Stage

2.4.3 Growth stage

This is the last stage in the process of forming thin layers, and it is considered a continuation of the coalescence process (Rahal 2013). Where the size of the islands increases and they get closer to each other to fuse the islands, forming a thin film or a thin

layer on the surface of the substrate and separating the islands by the grain boundaries (Figure 2.3).

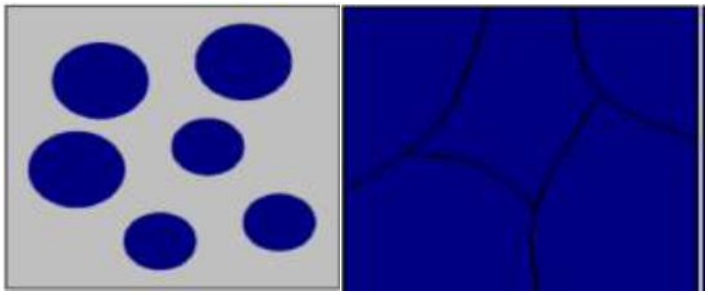

Figure 2.3 Growth stage

2.5 Thermal Adaptation

The process of exposing thin films to a certain temperature and for a specific period of time is known as thermal conditioning or heat treatment, and it may take place in a vacuum and in the presence of a certain gas. Crystal structure of the substance. The process of adaptation differs in its effects on the material according to the type of material and the conditions of the process, and is sometimes used to transform the thin layer consisting of one or more substances from a random state to a crystalline state (Wang *et al.* 2009).

2.6 Thin Film Deposition Methods

It is possible to deposit transparent carrier oxides in the form of thin films by many methods, and these methods are classified into two main categories: physical methods and chemical methods, as shown in the following Figure 2.4.

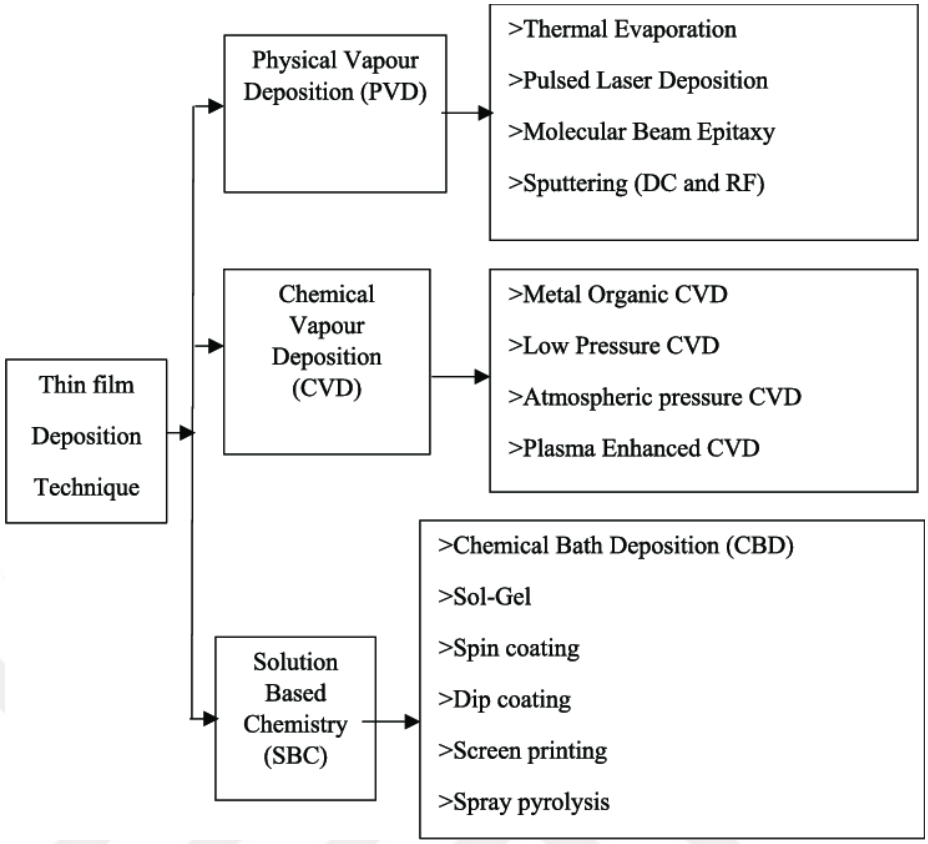

Figure 2.4 The methods of deposition of thin films (Wang *et al*. 2009)

2.6.1 Physical methods

2.6.2 Technique of physical vapor deposition

Thermal evaporation is a physical technique for preparing thin films under low pressure that may reach 10^{-4} bar. It requires evaporation of the metallic substance used in preparing the thin films from the original material, then concentrating the steam on the used substrate. What is known as a joule effect, magnetic induction, a beam of electrons with which a substance is ejected, or a laser beam, as we will see in the third method (Hafdallah 2007). This method is simple and does not need to pump a gas to form a plasma inside a vacuum because other physical methods need a plasma medium as a transport medium (Hussein *et al.* 2017). And with some special difficulties in this method, such as the difficulty of placing more materials with low pressure vapors, and there are difficulties in forming chemical compounds in the case of a bimetallic mixture to form thin films. The

compound can expand and change its phases due to heat or the interaction of the substance in the case of steam with the carrier of the original material and interactions with the diffuse gases can occur during heating, and there are other difficulties when heating with an electron beam or a laser beam (Figure 2.5).

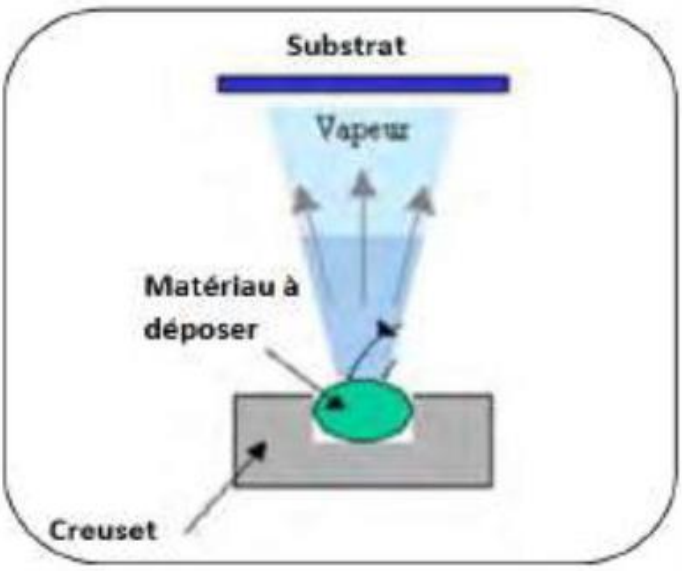

Figure 2.5 The thermal evaporator (Hafdallah 2007)

2.6.3 Vacuum evaporation

This method is considered one of the appropriate methods through which distinctive properties of the formed film can be obtained. The films are prepared by placing the matter to be evaporated in a basin and under very low pressure less than 10^{-4} bar and sometimes reaching 10^{-9} bar (Biswal *et al.* 2014). As these pressures vary according to the materials used to prepare the films, then the material is heated to the melting point by passing a high-intensity electric current, and this method is suitable for evaporating most metals and semiconductors as shown in the following Figure 2.6.

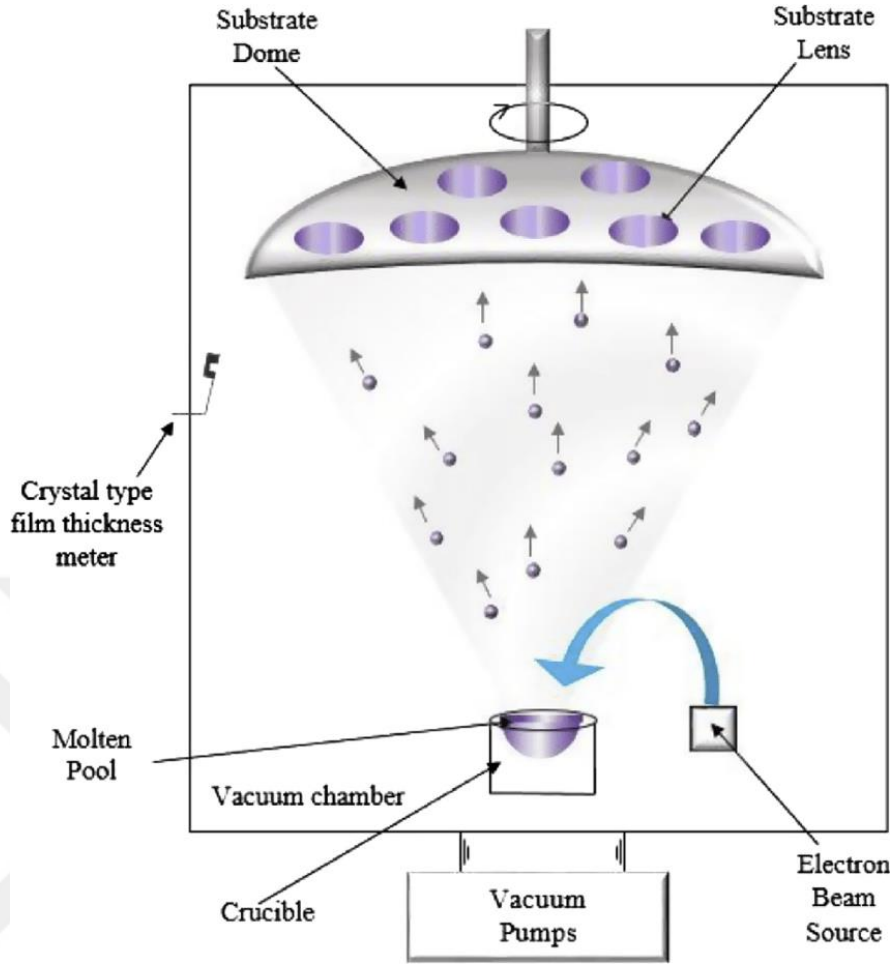

Figure 2.6 Thin-film deposition by vacuum evaporation method (Biswal *et al*. 2014)

2.6.4 Laser ablation technique

The principle of extraction or heating with a directed laser beam as shown in the Figure 2.6 below, the process is done by preparing the laser beam and then passing through the vacuum to reach the surface of the metal used as a source for preparing thin films, which absorbs the beam at a value of the necessary energy focused on the metal, fragmentation or fragmentation of the outer surface atoms occurs and turns into atoms In the form of steam due to the large thermal energy of the laser beam, this energy is related to the wavelength of the beam and the pulse or frequency of the incident beam, and it is most often between (10-50 MW/cm^{-2}) in the ultraviolet laser (Figure 2.7).

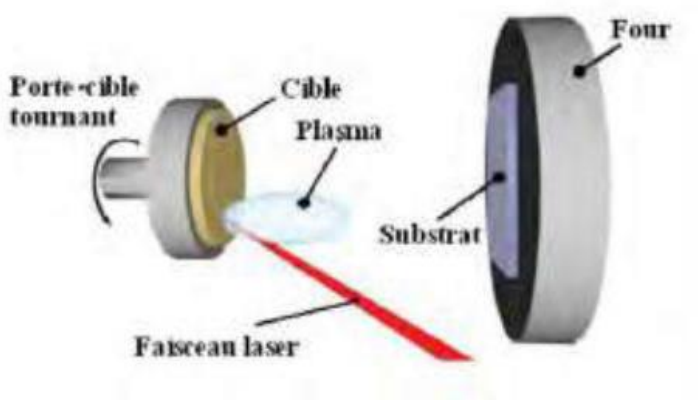

Figure 2.7 Laser ablation technique (Rahal 2013)

2.6.5 Chemical methods

2.6.6 Chemical vapor deposition technique (CVD)

This method is used in a large number of fields, including the great use in the field of semiconductors. In this method, gases react chemically with the surface of the heated substrate in order to form a thin, solid layer on the surface of the substrate. In order to activate the chemical reaction, the temperature of the substrate must be between 500 °C To 2000 °C and according to the nature of the precipitate. The method requires a high temperature to meet the reaction needs (activation energy), while industrial needs prefer low temperatures, so this method suffers from improvements to reduce the temperature, and we mention from these methods:

- Chemical vapor deposition by plasma assisted (PACVD)
- Chemical vapor deposition by low pressure (LPCVD)
- Chemical vapor deposition by ultra-high vacuum (UHV-CVD)

2.6.7 Sol-gel technique

Thin films are placed in a (gel-liquid) method, and this is in two different forms: the deposition method by (dip-coating) and the deposition by (spin-coating) as shown in the Figure 2.8.

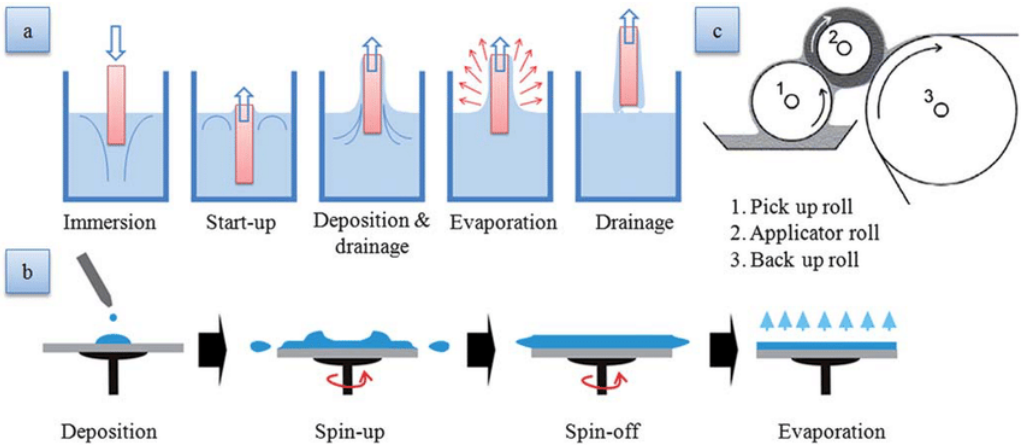

Figure 2.8 (a) dip coating and (b) spin coating technique

A. Deposition by dip coating

This technique depends on dipping the slide or substrate and pulling it under specific and fixed conditions in order to obtain a thin slice of uniform thickness, so that the liquid covers the slide and the layer is uniform and porous as shown in the Figure 2.9. This method allows obtaining a thick layer by controlling the concentration of the solution and a number of layers when adequate heat treatment is provided (Kim *et al.* 2008). The gelatinous solution (sol-gel) technique is one of the preferred techniques because it is characterized by low cost and low chemical precipitation loss, as well as the suitability of this method for large surfaces (Yi *et al.* 1988). This will be the method used in this research. for the production of thin films.

B. Deposition by spin coating

In this method or technique, drops of the solution that we want to be deposited are placed on the slide used as a substrate, then a high speed of rotation is applied to remove the excess liquid by the method of continuous rotation, and from it the layer becomes homogeneous at all points. This method aims to obtain a homogeneous thin layer with a fixed thickness. With reference, the thickness of the obtained layer must be at least 200 nanometers so that there is no imbalance in its diagnosis (Kamal *et al.* 2004).

C. Sedimentation system of spray pyrolysis technique

It is a technique that relies on spraying the solution containing the atoms of the substance to be prepared thin films, using air pressure in the form of a spray on the surface of the heated substrate, so that the chemicals interact to form a solid layer. Of varying thickness, and its production method is also considered simple and inexpensive (Benhaoua *et al.* 2014). This method is used to deposit dense thin layers, porous layers, as well as to produce powder or multiple layers on top of each other, as this flexible technology has been used for several decades in the glass industry and the production of solar batteries (Figure 2.9).

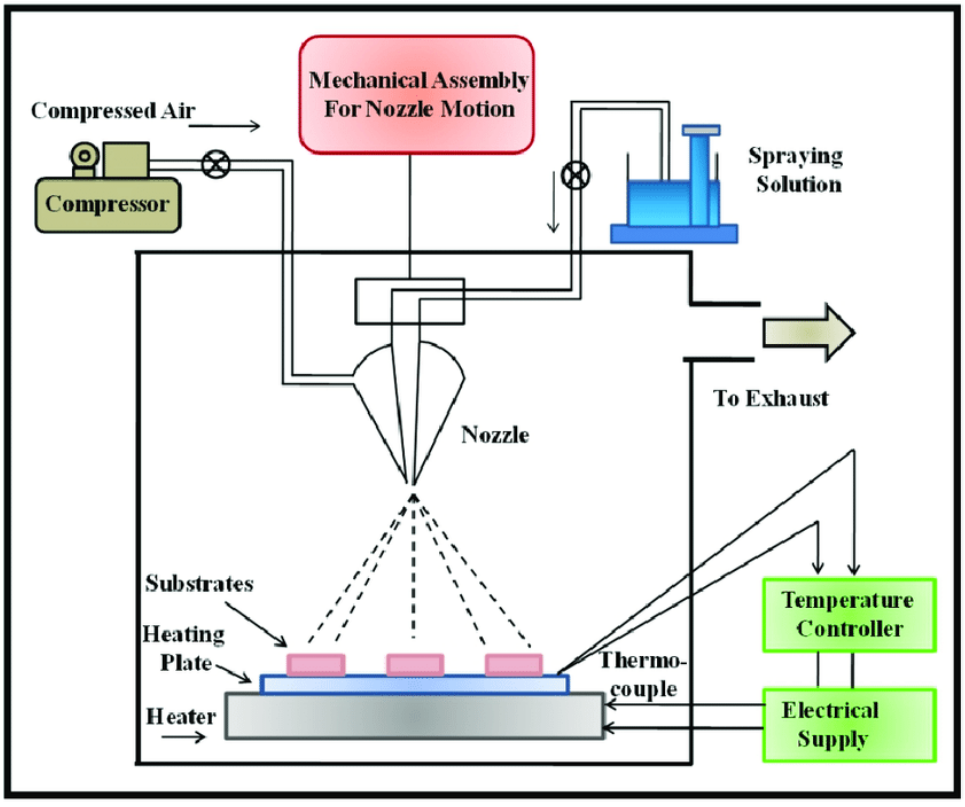

Figure 2.9 Schematic of spray pyrolysis technique and its equipment (Benhaoua *et al.* 2014)

2.7 Criteria for Selecting the Appropriate Deposition Technology

Recently, studies have relied widely on the use of different techniques for deposition of transparent carrier oxides (TCO) films. The growth mechanism plays a major role in influencing the different physical properties of thin films. Because the deposition of the same material with two different techniques does not provide the same results and usually have different physical properties, and actually all reasons of that is the electrical and optical properties of these thin films depend largely on the structure and morphology as well as the nature of the impurities present. This means that a comprehensive and detailed study must be conducted on the relationship between the properties of films and different deposition techniques. There are many techniques that contribute to the growth of thin films of transparent carrier oxide (Wang *et al.* 2009).

2.8 Thin-Film Sampling Techniques

There are several techniques for examining thin films, where the latter enables us to identify all physical properties, including structural and morphological properties, optical and electrical properties of the prepared films, and we will address some of these techniques in the following paragraphs.

2.8.1 Thin film thickness measurement

Measuring the thickness of films is among the most important necessary constants, as it is used to determine several other constants such as the absorption coefficient, resistivity etc. One of the simplest ways to estimate the thickness of the films is to use the gravimetric method and this is according to the following relationship (Khan *et al.* 2011) Equation (2.1).

$$d = \frac{\Delta m}{\rho s} \tag{2.1}$$

d: Thin film thickness

Δm: Mass difference before and after sedimentation

P : Thin film density

S: Thin film surface area

The thickness of the samples can also be calculated directly by inspecting the MEB scanning electron microscope, and it can also be calculated from the transmittance spectrum using two methods (Figure 2.10).

- Least squares method: This method uses (Fit) software through some values in the transmittance spectrum.
- Interference fringe Method: It is based on information from the transmittance spectrum in the visible spectrum to the infrared spectrum.

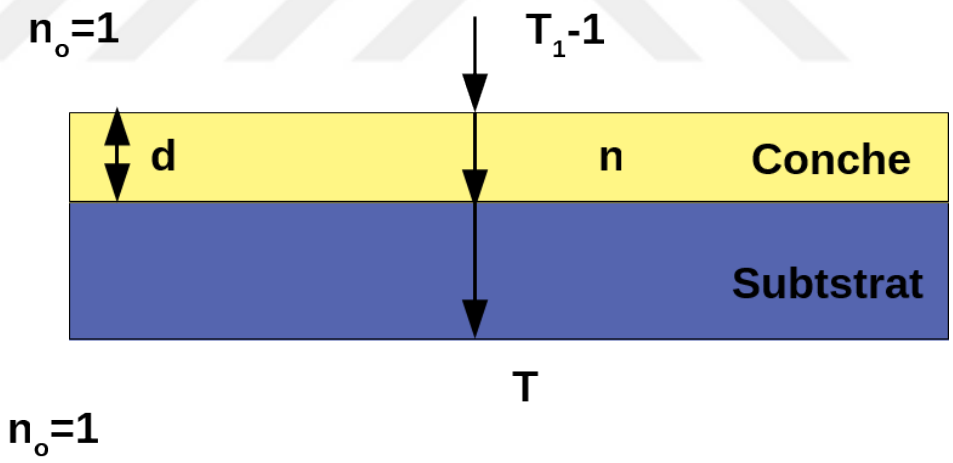

Figure 2.10 Layer system on a transparent substrate

The transparent substrate is thicker than the thickness of the layer (d) it has a refractive index (s) and a permeability index $\alpha_s = 0$ and a refractive index of air ($n_0 = 1$). (T) and (α) the permeability and absorption coefficient of the thin layer and (n) the refractive index of the layer thin, if the thickness (d) is uniform we get the spectrum shown in the following Figure 2.11.

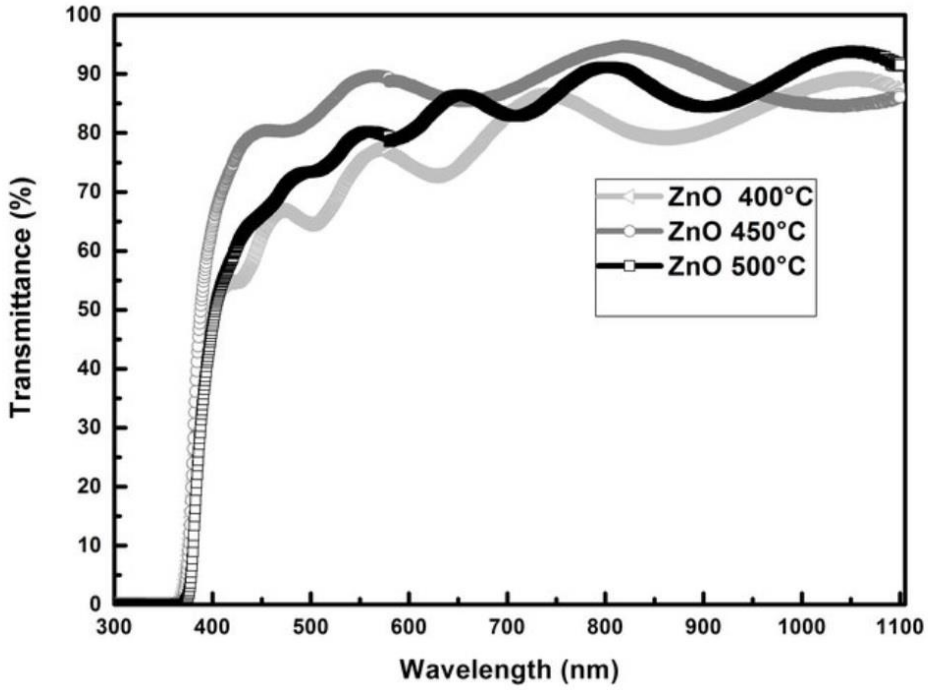

Figure 2.11 The permeability for thickness calculation of thin films (Kim *et al.* 2008)

Since the layer has an uneven surface and a smooth surface in contact with the substrate, the refraction of the rays between the surface contacting the substrate and the upper surface of the layer (Khan *et al.* 2011). The transmittance between two values, one is minimum and the other is maximum, and in terms of wavelength λ_1, λ_2, the thickness of the film is given by the following Equation (2.2).

$$\mathbf{d} = \frac{\lambda_1 \lambda_2}{2(\lambda_1 n_2 - \lambda_2 n_1)} \tag{2.2}$$

2.8.2 Structural features

2.8.3 X-ray diffraction

The X-ray diffraction technique has widely used in determining the structural properties of solid objects. This technique is characterized as non-destructive to the structure of the sample. It allows to attain information about the crystalline structure of the sample. When

X-rays interact with the pure crystalline material, we obtain a diffraction pattern that represents a distinctive fingerprint of the material. As shown in the corresponding (Figure 2.12). When single-wavelength X-rays are shined on the surface of a thin film, peaks of reflections called Bragg reflections will appear on the crystal surfaces at specific diffraction angles. This method enables us to obtain information about the crystal structure as well as to calculate some crystal constants such as Crystal lattice constants, grain size ratio, stresses, etc., (Figure 2.12).

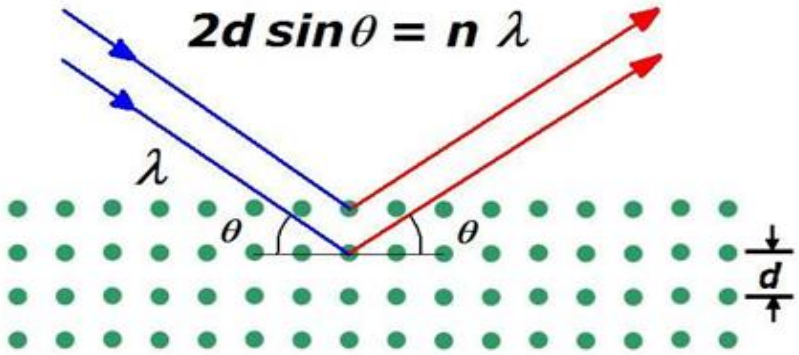

Figure 2.12 The diffraction of X-rays as they fall on the crystal (Rahal 2013)

Bragg's law is given by the Equation (2.3).

$$2d\sin\theta = n\lambda \quad (2.3)$$

d = Represents the distance between crystal planes.

θ = diffraction angle.

λ = X-ray wavelength.

n = is an integer representing the order of the reflection.

2.8.4 Determination of the constants of the crystal structure

From the bragg's equation and other equations, the following can be extracted from the cell dimensions in the hexagonal parapet, according to which the zinc oxide crystal crystallizes, for example. The Equation (2.4) for calculating the constants of the crystal cell is also given (Khan *et al.* 2011), Equation (2.4).

$$a = \frac{\lambda}{\sqrt{3}\sin\theta_{(100)}} \qquad c = \frac{\lambda}{\sin\theta_{(002)}} \tag{2.4}$$

2.8.5 Raman spectroscopy

Raman spectroscopy is one of the modern techniques that took a long time to develop compared to infrared spectroscopy, until it witnessed a great development at the end of the eighties and the beginning of the nineties and it had many and varied applications that included many scientific fields: physical, chemical, biological, medical, etc. The use of Raman microscopy and optical fibers in this spectroscopy made it an effective tool in analytical chemistry and contributes to solving many problems, especially in the detection of chemical compounds and knowledge of their structure and properties (Hafdallah 2007).

2.8.6 Working principle of raman spectroscopy

The principle of the Raman spectroscopy device is to excite the material to a high energy level with a monochromatic laser beam of light, which produces radiation that the device picks up with sensitive sensors after passing through filtering strips, the latter of which results from the so-called Rayleth diffusion or soft diffusion, and It consists of two types of signals, the first is called Raman-Stokes and the second is Raman-Stokes antigen. It is the most widely used and it can be explained how to stimulate or excite the electronic layers in the atoms after absorbing the energy of the photons by the atoms, and this results in the emission of two types of radiation as we mentioned previously, through which we obtain the Raman spectrum (Figure 2.13). And the two molar figures, one of them shows

the energy change between incoming and outgoing, and the second is the path of the rays in the device and their passage through the diagnosed sample (Figure 2.14).

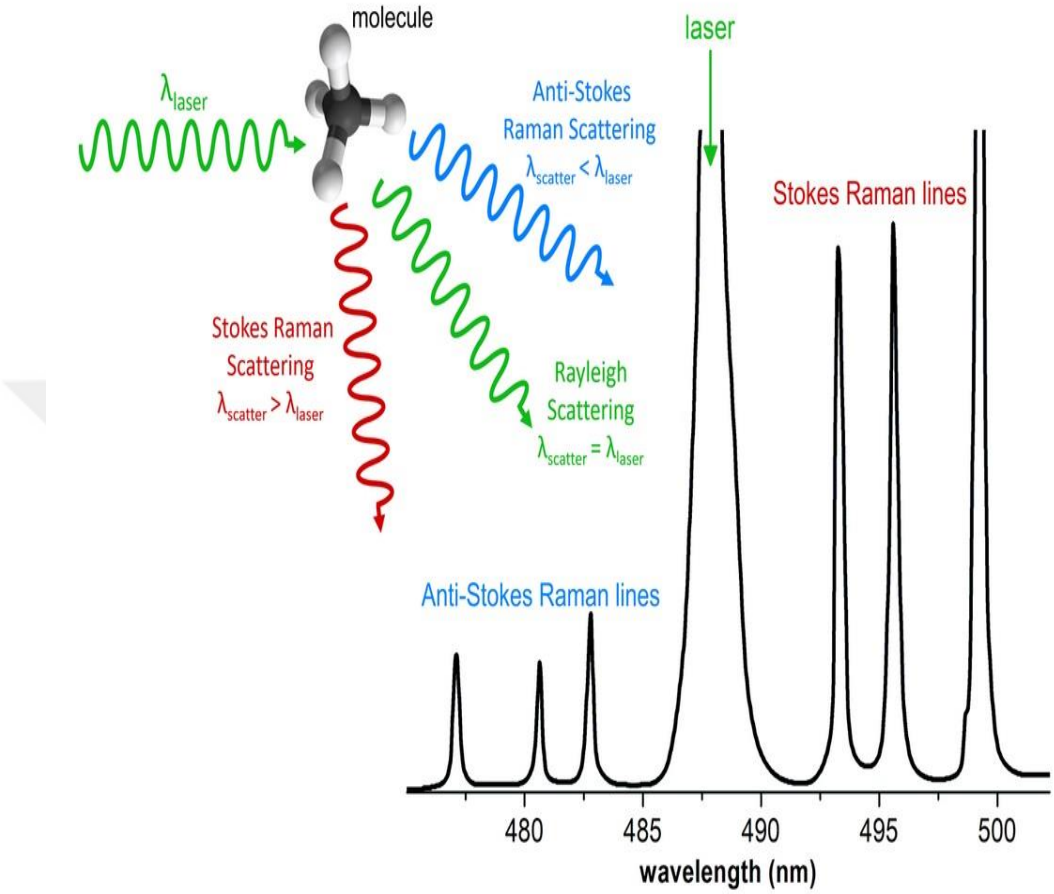

Figure 2.13 The absorption and emission of high energy rays (Hafdallah 2007)

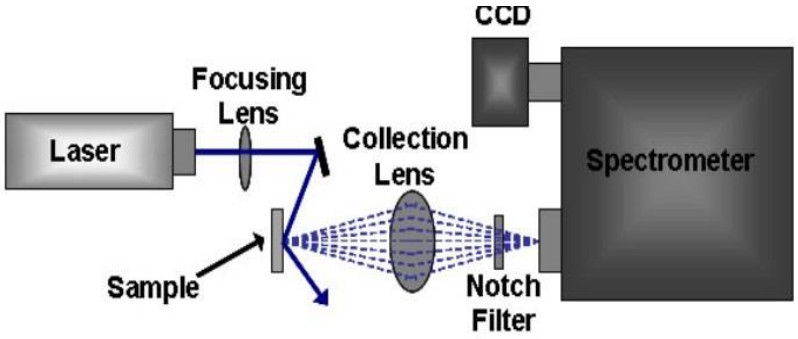

Figure 4.3.5 Schematic of a macro-Raman spectrometer.

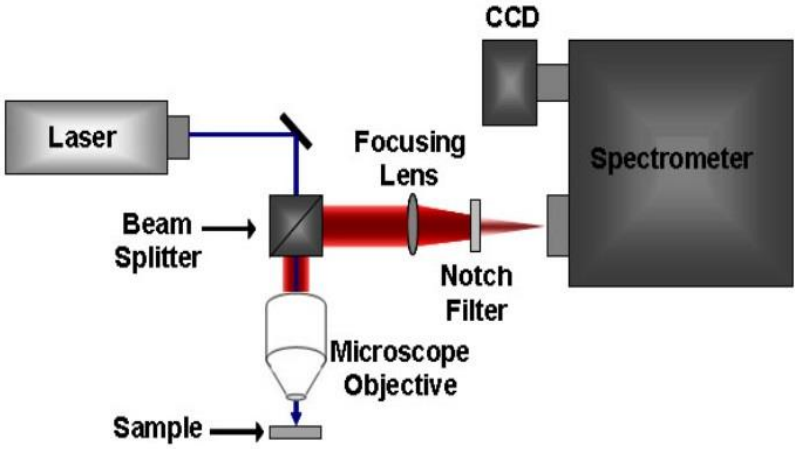

Figure 2.14 The working principle of raman spectroscopy

2.8.7 Diagnosis using a scanning electron microscope

Electron microscope that produces images of a sample by scanning that area with a focused beam of electrons is a scanning electron microscope. The electrons interact with the atoms in the example, generating various signals that involving information about the topography and composition of the surface. The electron beam has usually scanned using raster scanning and the location of the beam which is combined with the signal to produce an image. Images of the order of (0 nm) can also be obtained. Samples can be viewed at high vacuum, at low vacuum, and at a wide range of very low or high temperatures. The most common scanning electron microscopy technique is to determine secondary electrons emitted from excited atoms by an electron beam and then an image is generated showing the topography of the surface (Figure 2.15).

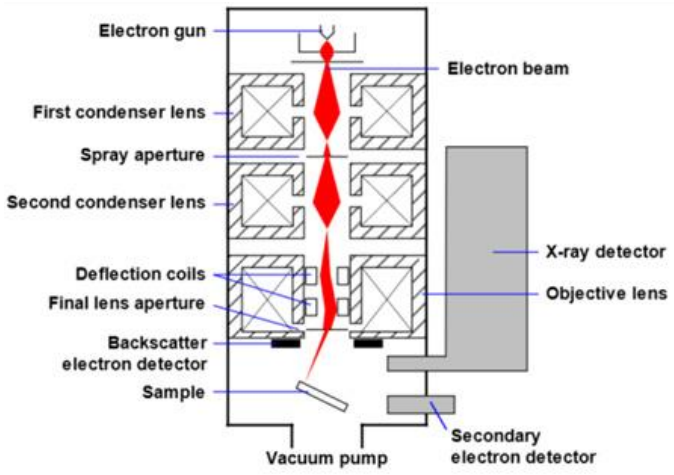

Figure 2.15 The components of a scanning electron microscope (Zhou *et al.* 2006)

2.8.8 Infrared spectroscopy (IR)

The technique of analysis by infrared spectroscopy is one of the most important methods of analysis currently used. It depends on absorption spectroscopy, where this spectroscopy is used to determine the chemical groups in the compounds to be studied. They are widely used in chemical analysis. By means of infrared spectroscopy, it is possible to distinguish between compounds.

2.8.9 Working principle of infrared spectroscopy

Molecules naturally vibrate in the form of vibration patterns, but with very weak amplitudes. If the frequency of the incoming photon matches the frequency of vibration of the normal patterns of the molecule, the molecule will respond to it directly. In other words, a photon whose energy is equal to the energy required for the molecule to pass from a low energy state to an excited state is absorbed and its energy is converted into vibration energy. The diagram represented in the corresponding figure summarizes this phenomenon (Figure 2.16).

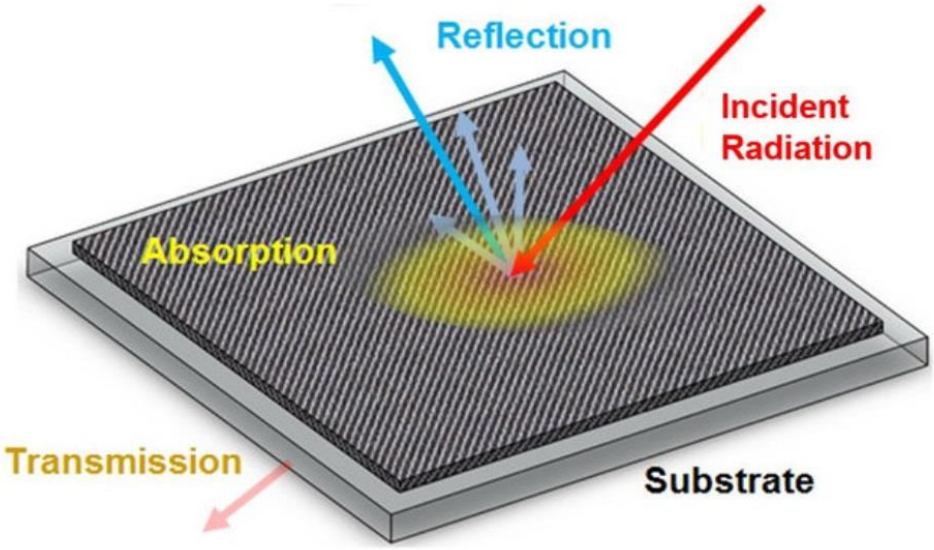

Figure 2.16 The absorption of infrared rays

The absorption of some of the incoming photons cause to the appearance of coincidence lines for the absorbed photons in the infrared spectrum of the molecule. This absorption characterizes the bonds between atoms, since each mode of vibration corresponds to a single movement of the molecule if there is a direct correspondence between the frequency of the absorbed radiation and the structure of the molecule (Kamal *et al.* 2004). The figure shows the components of an infrared spectrophotometer (Figure 2.17).

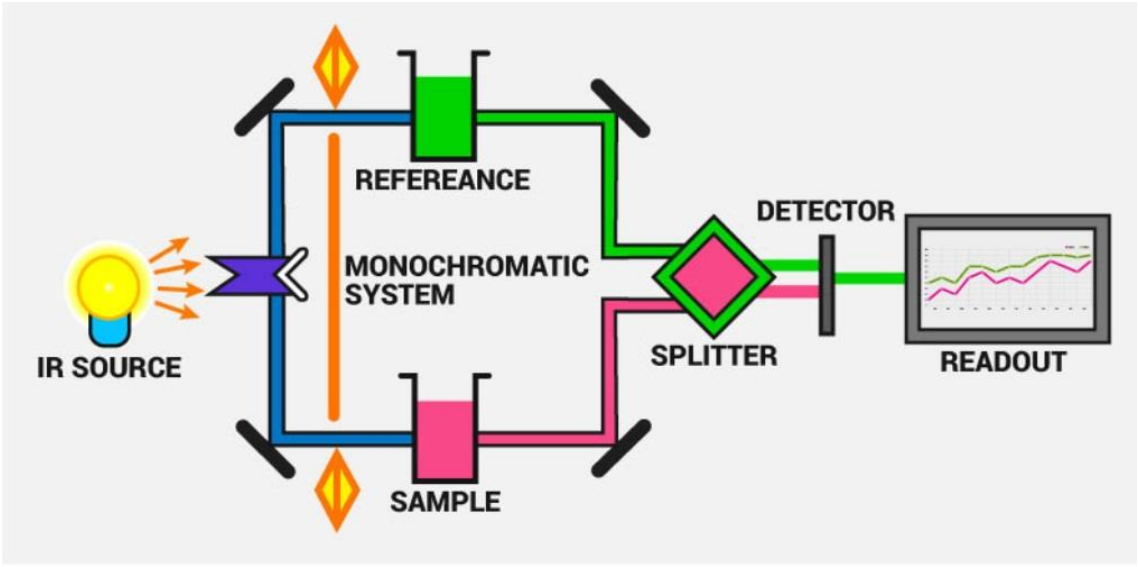

Figure 2.17 The components of an infrared spectrophotometer

3. MATERIALS AND METHODS

This chapter deals with the practical side and includes a general description of the devices used and the factors (Sn) (ZnO) at work and the way to prepare the membrane that affects the way to prepare these membranes, the devices used to diagnose their nature, and the measurements that were conducted on them.

3.1 Instruments

3.1.1 Scanning electron microscope (SEM)

The scanning electron Emitted electrons are used in a microscope. The scanning electron microscope operates on the idea of using kinetic energy to generate signals on the interaction of the electrons. These electrons have used to observe crystallized elements and photons. They are secondary electrons, backscattered electrons, and diffracted backscattered electrons. Images have created using secondary and backscattered electrons. While the backscattered electrons demonstrate contrast in the composition of the specimen's elements, the secondary electrons that have emitted from the specimen serve as the primary means of detecting the morphology and topography of the specimen (Figure 3.1).

Figure 3.1 Hitachi SU 5000 field emission scanning electron microscope

3.1.2 APD 2000 PRO-XRD device

APD 2000 PRO diffractometer is a high power - Theta/2Theta - laboratory powder X-ray diffractometer equipped with all the most modern technical properties which grant accuracy, precision, safety, and easiness of use for XRD analysis of polycrystalline materials. Due to a wide offer of configurations and accessories such as a high-speed detector, scintillation counter, high-low temperature, and humidity chamber, secondary monochromator, spinner, and multiple sample holder, APD 2000 PRO is a powerful tool for powder diffraction applications such as routinary qualitative and quantitative phase analysis, non-ambient analysis, structure solution and refinement, crystallite size and degree of crystallinity calculation (Figure 3.2).

Figure 3.2 APD 2000 PRO-XRD device

3.1.3 UV-VIS spectrometer

When ions, atoms, or molecules in a sample transition from one energy state to another, a process known as spectroscopy is used to detect and analyze the electromagnetic radiation that is emitted or absorbed. is a sort of absorption spectroscopy that makes use of light from the electromagnetic radiation spectrum's neighboring visible and UV ranges. The principal absorption wavelength varies from 100 to 700 nm (Figure 3.3).

Figure 3.3 UV-VIS Spectrometer

3.1.4 Annealing oven

Heat treating, often known as heat treatment, is a series of industrial, thermal, and metallurgical procedures used to change a material's physical, and occasionally chemical, characteristics. Metallurgical applications are the most typical. Numerous additional materials, including glass, are produced via heat treatments. In order to accomplish the desired outcome, such as the hardening or softening of a material, heat treatment typically entails heating or cooling to extremely high temperatures (Figure 3.4).

Figure 3.4 Annealing Oven

3.2 SILAR Method

With the SILAR method, they can be obtained around room temperature with various base materials such as semiconductors, insulators, and metals. Since the production takes place at low temperatures, the possibility of oxidation and corrosion is very low. In order to obtain high-quality films with the SILAR method, parameters such as solution densities, pH values of the solutions, waiting times of the material to be formed in the solution and the number of rounds should be well optimized. As a result of many years of research, it has been proven that the physical properties of the films obtained thanks to

these various parameters of the SILAR method can vary greatly (Pathan and Lokhande, 2004).

The SILAR method is a newer and less researched method compared to other methods. It was first performed by Ristov in 1985. Nicolau gave the name SILAR to this method in 1985. Nicolau et al. obtained ZnS, CdZnS, and CdS thin films with this method. SILAR method I-VI, II-VI, III-VI, V-VI, VIII-VI 2 chalcogen groups I-III-VI, II-II-VI, II-III-VI, II-VI-VI and II-VI. It is used in thin film coatings of V-VI three chalcogen groups (Pathan and Lokhande 2004).

The SILAR method emerged as a result of the development of the chemical bath method. The Chemical Bath Storage (CBD) method is a method obtained by immersing clean substrates in aqueous solutions containing a metal ion source, hydroxide, sulfur, or selenite for a certain period of time and depositing semiconductor films on these substrates. The SILAR method has many advantages over other methods. these;

i. It is easy to form a film by using a cationic solution prepared in certain proportions.
ii. Unlike the closed steam doping method, which requires a high-quality substrate and vacuum at every stage, these conditions are not sought in the SILAR method.
iii. The thickness of the film to be coated can be easily adjusted by changing the coating ratio and the number of cycles.
iv. Coating can be performed on less durable materials as the coatings take place at room temperature.
v. Unlike high energy methods such as the radio frequency magnetron sputtering (RFMS) method, it does not cause harmful heating for the precipitated material.
vi. There are no limitations to the substrate material surface profile and dimensions.

Other than these features, the SILAR method is a cheap, simple, and useful method for precipitation in a large area. Semiconductor films are deposited in glass beakers. Starting materials are the most easily available and inexpensive materials. Since it is a chemical method, a wide variety of substrates can be used. Thus, it will be a suitable substrate for

any precipitation where the solution can easily reach. To avoid corrosion or oxidation of the base materials, precipitation is carried out at or near room temperature.

3.3 Obtaining ZnO Semiconductor Films by SILAR Method

ZnO films were prepared by immersing them in solutions prepared in glass beakers on the microscope glass bases for a certain period of time. After the prepared films were dried, their structural and optical properties were investigated.

3.3.1 Cleaning glass ceilings

Microscope glass bases measuring 15 mm x 75 mm x 1 mm were used to obtain ZnO semiconductor films. Glass bases were first rinsed with deionized water and boiled in detergent water. It was then cleaned with acetone and ethanol. Finally, they were kept in 30 % nitric acid and 30 % sulfuric acid solutions for one hour, rinsed with ultra-deionized water at each stage, and dried in an oven.

3.3.2 Preparation of solutions

Two separate solutions were prepared to obtain ZnO films. The first solution; 0.1 M zinc nitrate (Zn $(NO_3)_2$) solution was prepared by dissolving it in 100ml ultradeionized water. Then ~5 ml of ammonium hydroxide ((NH_4) OH) was added to make the solution alkaline (until the pH value was about 12). The second solution was prepared by dissolving 1 mL of 28 % hydrogen peroxide (H_2O_2) in 100 ml of ultradeionized water. Both prepared solutions were placed in separate beakers. Maximum 220 g for weighing operations. can weigh 0.1 mg precision SHIMADZU AY 220 model electronic balance is used.

3.3.3 Experimental procedure

In order to perform the SILAR experiment, the glass bases are left immersed in the zinc nitrate solution for 30 seconds to absorb the zinc compound. Then, when it is immersed in a hydrogen peroxide solution and held for 40 seconds, the reaction occurs on the glass base and the form of zinc oxide is formed. And so, the SILAR experiment happens. The films were repeated for approximate numbers 5, 7, 10, 20, 25, and 30. The period of glass substrates in zinc solution is called the adsorption period, and the period in hydrogen peroxide solution is called the reaction period. In order to remove the hydroxyl (OH^-) phase from the obtained films, they were dried in air at 400 °C for 60 min. The Nabertherm brand oven was used for the drying process.

3.3.4 Formation of ZnO Films

The ZnO formation mechanism occurs as follows. Liquid ammonium is added slowly to make the 0.1 m Zn $(NO_3)_2$ solution used as a zinc source alkaline. When ammonium is first added, $Zn(OH)_2$ is formed as an ionic product, which makes the solution look milky. This reaction is expressed as follows Equation (3.1):

$$Zn(NO3)_2 + 2NH_4OH \rightarrow Zn(OH)_2 + 2NH_4^+ + 2NO^- \quad (3.1)$$

However, when enough NH4OH is added, Zn^{+2} ions in the environment are reduced and Zn $(NH_3)_4^{+2}$ is formed. Thus, precipitation in the solution is avoided. In addition, the solution takes on a clean and transparent appearance, Equation (3.2):

$$Zn(OH)_2 + 4NH_4^+ \rightarrow Zn(NH_2)_4^{+2} + 2H_2O + 2H^+ \quad (3.2)$$

When immersed in the solution defined by the glass bases, the zinc mixture ions adsorb on the glass base with the help of attractive forces. These forces can be defined as molecular attraction or Van-der Walls forces. Then, when the glass bases are immersed in the hydrogen peroxide solution at room temperature, a ZnO semiconductor film is formed on the surface as a result of their reaction. Here, H_2O_2 solution is used as hydroxyl

source. It was observed that the obtained ZnO films formed on both surfaces of the microscopic glass substrates and were homogeneous. In order to determine the structural and optical properties of the semiconductor films, the film on one surface of the glass substrates were cleaned with nitric acid. Glass bases, one surface of which is film-coated, are prepared for measurement Equation (3.3) and Equation (3.4):

$$H_2O_2 + H_2O \rightarrow 2OH^+ + 2H^+ + 1/2O_2 \quad (3.3)$$

$$Zn(NH_3)_4^{+2} + 2OH^- \rightarrow ZnO + 4NH_3 + H_2O \quad (3.4)$$

3.4 X-Rays Methods

Experimentally, Bragg's law can be used in two ways. Using an X-ray of known wavelength λ, the angle θ is measured and the distance between planes in the crystal structure can be determined. On the other hand, the wavelength λ of the radiation used can be determined by measuring the angle θ with the aid of a known interplanetary crystal. In addition, crystal structure analysis can be performed by measuring the intensity of Bragg reflections. The general structure of a spectrometer used in X-ray structure analysis is shown in Figure 3.5. X-rays from the source are sent on the sample, which can be placed at the desired angle relative to the incoming beam by rotating it around an axis passing through the center of the spectrometer. The detector is an ionization chamber or any counter that measures the intensity of diffracted X-rays and can be rotated around the center by turning it into the desired angular state. When the sample is placed such that the angle between the reflector planes and the incident beam is θ, the detector is placed in the 2θ position. Thus, the distance between the crystal planes versus the intensity of the diffracted beam is measured at varying 2θ angles.

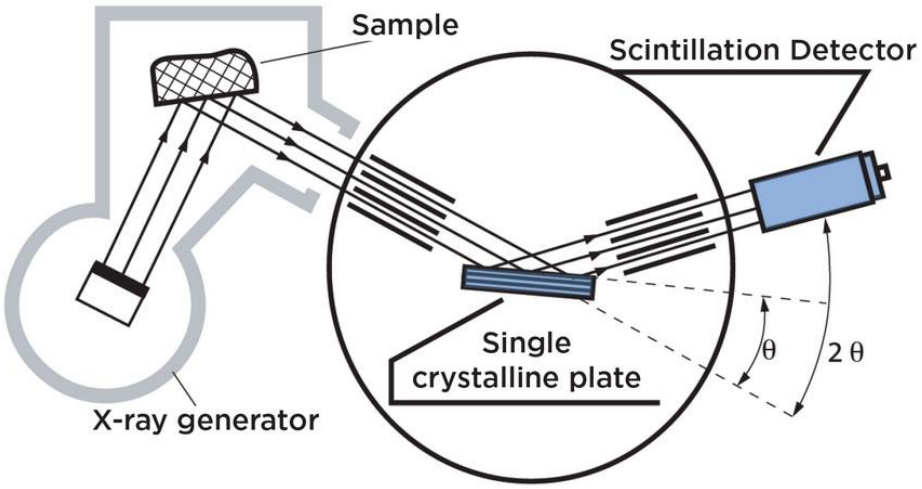

Figure 3.5 X-ray spectrometry

Diffraction occurs when the Bragg condition is satisfied. Equation (3.5) establishes the limiting conditions for λ and θ for any crystal. If a single crystal is arbitrarily placed in an X-ray beam with monochromatic radiation, no diffraction beam is generally produced. X-ray diffraction data can be determined using three different diffraction methods whose working principles are based on Bragg's law. The differences between these methods are due to the beam and sample used. These methods are; the rotating crystal method, powder method, and Laue method. In the rotating crystal method, single crystal and fixed wavelength rays are used as samples. In this method, varying values are obtained for the Bragg angle (θ). In the powder method, single wavelength rays are used with polycrystalline or powdered samples. Bragg angle θ is variable. In the Laue method, a single crystal and varying wavelengths are used as samples. In this method, the Bragg angle θ is kept constant. Of these three methods, only the powder method is used in the examination of polycrystalline materials. In this method, diffraction patterns are obtained depending on the intensity of the rays and varying angles. The d_o distance is calculated according to the angle values of the obtained peaks and the crystal structure is determined.

$$2d_o \sin\theta = n\lambda \qquad (3.5)$$

3.5 Absorption in Semiconductors

The most important absorption event in semiconductors occurs when an electron absorbs a photon and passes from the valence band to the conduction band. This event is called the fundamental absorption event. Basic absorption, which manifests itself as a rapid increase in absorption, is used to determine the energy range of the semiconductor (Lee 2003).

In the basic absorption event, an electron passes from the valence band to the conduction band by absorbing a photon from the incident light beam. As a result of this transition, a hall is formed in the valence band. In order for this transition to occur, the photon energy falling on the material must be at least equal to or greater than the forbidden energy gap of the semiconductor, Equation (3.5). Therefore, the frequency of the incident photon υ;

$$\upsilon \geq E_g / h \quad \text{veya} \quad \upsilon \geq \upsilon_0 \tag{3.6}$$

should be. Here; E_g is the forbidden energy gap h, is Planck's constant and C is the speed of light. $\upsilon_0 = \frac{Eg}{h}$ frequency is called the absorption limit.

The basic absorption spectra of the ZnO semiconductor films obtained by the SILAR method were obtained with Shimadzu UV-2450 Spectrophotometer in the 200 - 3300 nm scanning region. Using the basic absorption spectrum data of the films, a graph of $(\alpha h\upsilon)^{1/n}$ ~ hυ change was drawn for n =1/2, 3/2, 2, 3 values. Since the most suitable graphs are obtained at the value of n=1/2, the transitions are allowed direct band transitions.

3.6 Determination of Edge of Semiconductors by Absorption Method

The optical absorption method was used to determine the band gap of ZnO semiconductor films. The optical absorption method is widely used to determine band structures as well as to determine band structures of semiconductors. To find the forbidden energy gap of

the material by the absorption method $(\alpha h\upsilon)^{1/n} \sim h\upsilon$. The energy value of the point it cuts gives the forbidden energy range of that material.

4. RESULTS AND DISCUSSION

In this chapter, we review the results obtained by studying the structural and optical properties of ZnO films prepared by SILAR method, and studying the effect of impurity with tin and Cu-Sn on the properties of these films.

4.1 Energy Gap (E_g)

The energy gap gives a clear idea of optical absorption, where the membrane is transparent to radiation whose energy is lower in the energy gap ($h\upsilon < E_g$) and absorbent to radiation whose energy is greater than it ($h\upsilon > E_g$). It can be calculated through the relationship (Tauc), which depends on the graphic representation of the variables $(\alpha h\upsilon)^2$ in terms of ($h\upsilon$).

Table 4.1 shows that the values of the obtained energy gap changed by increasing the impurity ratio, reaching an energy gap of (3.35) when inoculating zinc oxide (ZnO) with a ratio of 3 % of Sn.

As this change gives an explanation that the grafting leads to the formation of new topical levels below the conduction band, and these levels are ready to receive electrons and generate tails in the energy gap that work towards changing the energy gap (Figures 4.1).

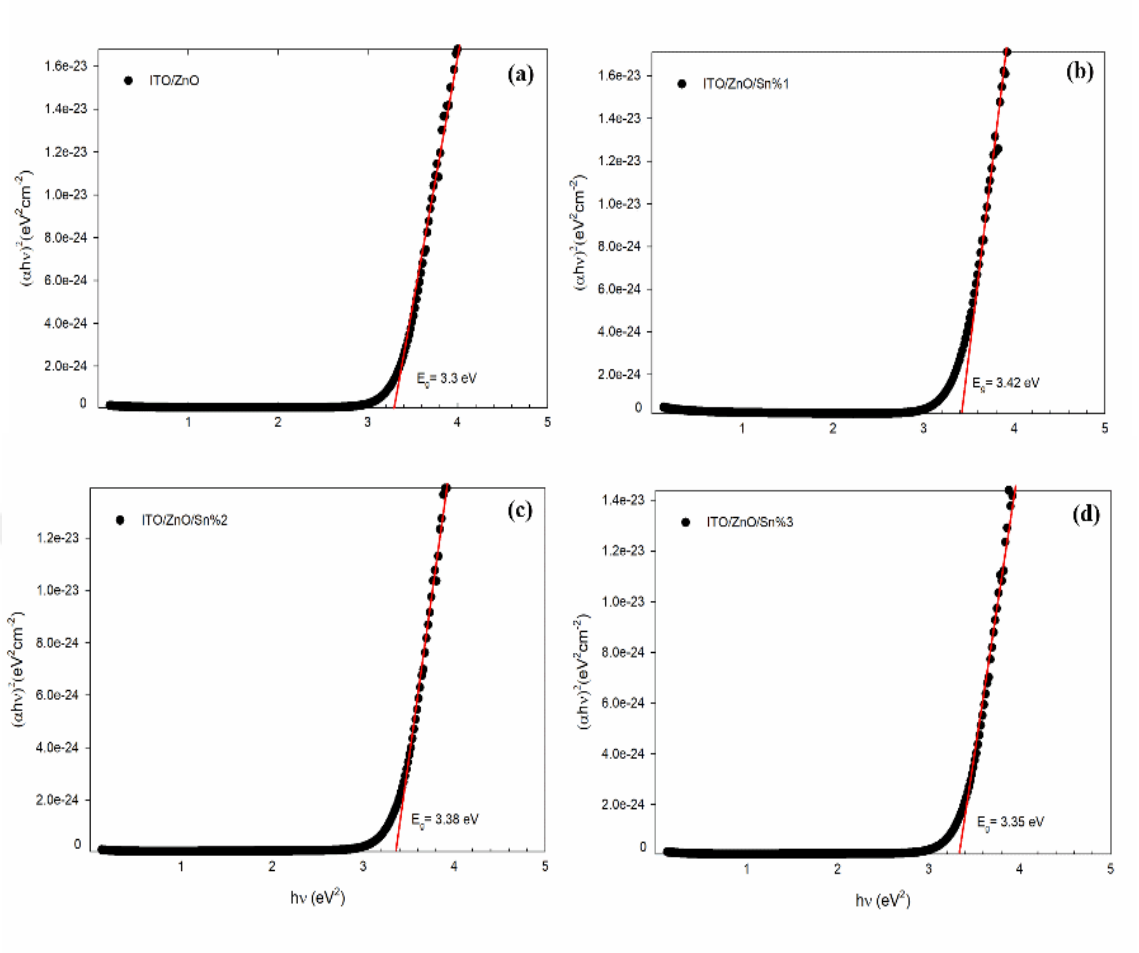

Figure 4.1 (a) ITO/ZnO, (b) ITO/ZnO/Sn 1%, (c) ITO/ZnO/Sn 2%, (d) ITO/ZnO/Sn 3% energy dependent band gap graphs of $(\alpha h\nu)^2$ $(eVcm^{-1})^2$ plotted using optical absorption measurements of thin films

Table 4.1 shows (a) ITO/ZnO, (b) ITO/ZnO/Sn 1%, (c) ITO/ZnO/Sn 2%, (d) ITO/ZnO/Sn 3% The forbidden energy values calculated from the hυ (energy) dependent graphs of $(\alpha h\nu)^2$ $(eVcm^{-1})^2$ drawn using optical absorption measurements of thin films are given. It was determined that the forbidden energy gap values of the produced thin film samples changed with doping.

4.2 Urbach Energy (Eυ)

Urbach energy (E_υ) was calculated by applying the absorption coefficient equation according to the relation: Equation (4.1).

$$\alpha = \alpha_\upsilon \exp(\frac{h\upsilon}{E\upsilon}) \quad (4.1)$$

From the results obtained and shown in Table 4.1, the values of the Urbach energy (E_υ) change with the change of the grafting network. Figure 4.2, shows the inverse proportion between the Urbach energy (E_υ) and the energy gap (E_g), as the Urbach energy increases with the increase of the grafting percentage. This is explained by the increase in the width of the local levels of impurities by increasing the inoculation, the Urbach energy is inversely proportional to the energy gap, and the latter decreases with the increase in the impurity rate, due to the increase in the number of carriers and the increase in absorption, which is consistent with previous studies.

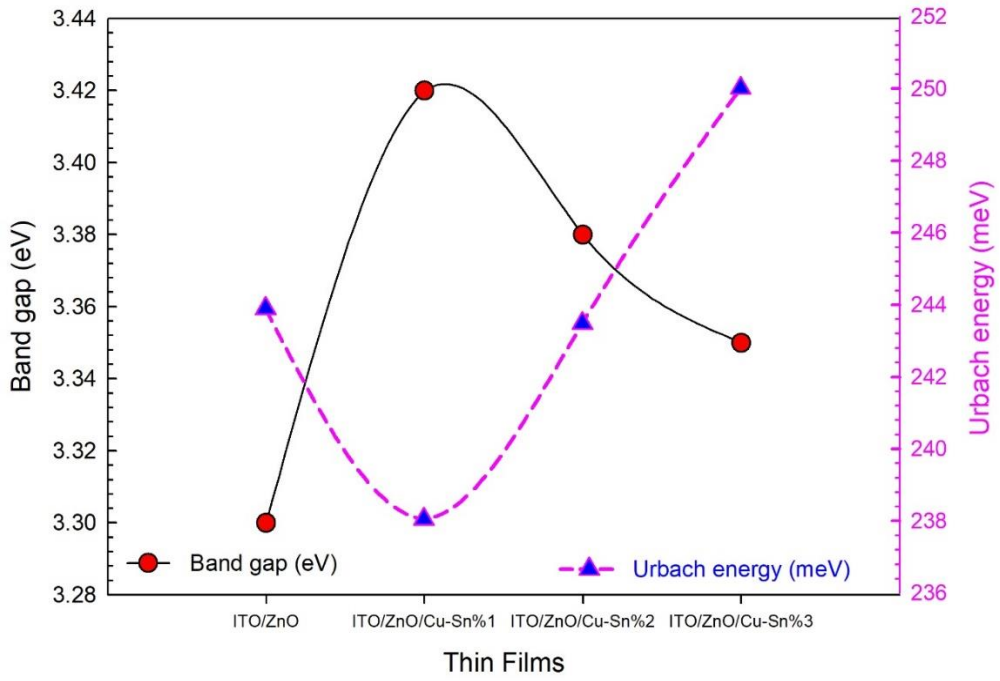

Figure 4.2 Band gap and Urbach energy versus of ITO/ZnO, ITO/ZnO/Sn 1%, ITO/ZnO/Sn 2%, ITO/ZnO/Sn 3% films

Table 4.1 shows the ITO/ZnO, (b) ITO/ZnO/Sn 1%, ITO/ZnO/S 2%, ITO/ZnO/Sn 3% plotted using optical absorption measurements of thin films $(\alpha h\upsilon)^2$ $(eVcm^{-1})^2$ with Forbidden energy (E_g) and Urbach (E_υ) values calculated from the connected graphs.

Table 4.1 Urbach (E_υ) values and forbidden energy (E_g) in ITO/ZnO, (b) ITO/ZnO/Sn 1%, ITO/ZnO/Sn 2%, ITO/ZnO/Sn 3%

Sample	**E_g (eV)**	**E_υ (meV)**
ITO/ZnO	3,3	243.90
ITO/ZnO/Sn 1%	3,42	238.05
ITO/ZnO/Sn 2%	3,38	243.48
ITO/ZnO/Sn 3%	3,35	250.01

4.3 Absorbance

Absorbance measurements were studied under the same conditions of permeability, where the graphic relationship of the absorbance was drawn as a function of the wavelength as in Figure 4.3. The results showed that the absorbance decreases gradually with the increase of the wavelength as well as the increase of the doping, as the charge carriers increase with the increase of the doping percentage.

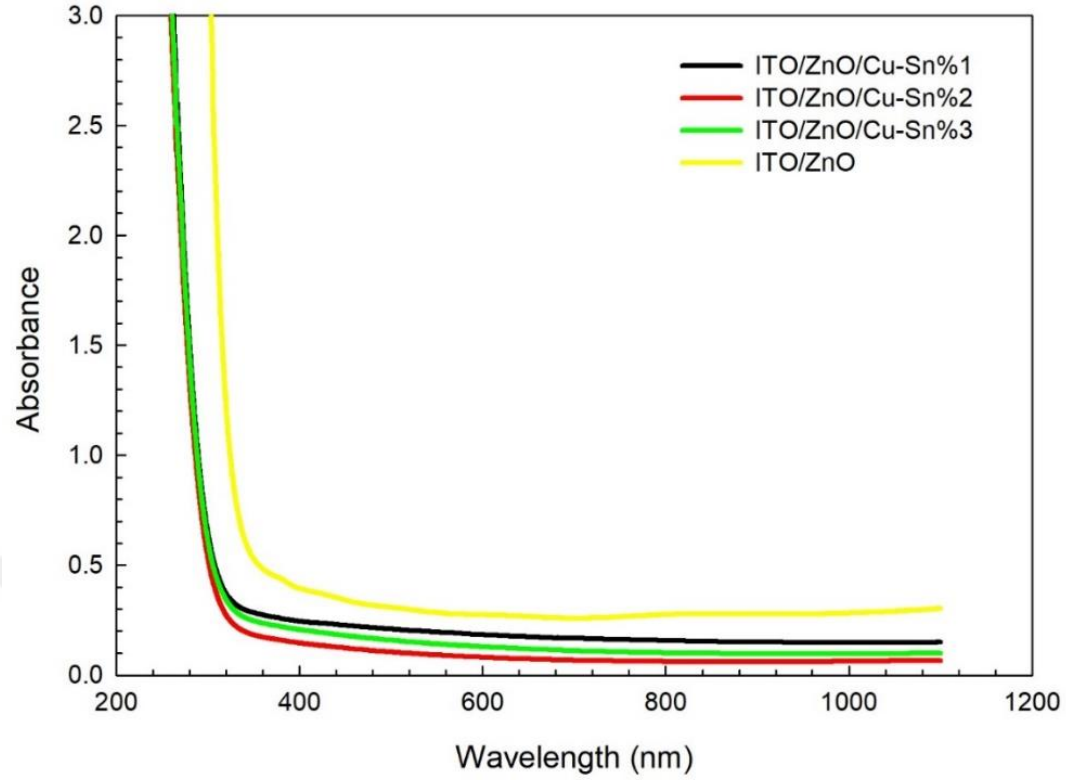

Figure 4.3 ITO/ZnO, ITO/ZnO/Sn 1%, ITO/ZnO/Sn 2%, ITO/ZnO/Sn 3% plotted using optical absorption measurements of thin films $(\alpha h\nu)^2$ $(eVcm^{-1})^2$ to energy connected graphics

4.4 Transmittance

Transmittance measurements were obtained within the range of wavelengths 200 - 1200 nm for all ZnO films prepared and inlaid with Cu and different ratios of Sn, 1 %, 2 %, 3 %, and the graphic relationship of the transmittance was plotted as a function of the wavelength placed in Figure 4.4. The results show that the transmittance increases with increasing the wavelength of all the membranes, as it was found that the value of the transmittance is the lowest possible in the ultraviolet wavelengths region of the spectrum within the range 300 - 400 nm and the transmittance begins to increase gradually with the increase of the wavelength in the visible region 400 - 700 nm, and we note that the transmittance values are almost constant in the near infrared region from 60 % to 84 %, and the transmittance increases at the inoculation ratio 2 % and decreases at the ratios 1 %, 3 %, due to the formation of levels of impurities. Inside the energy separator, which leads to an increase in absorbance and thus a decrease in transmittance.

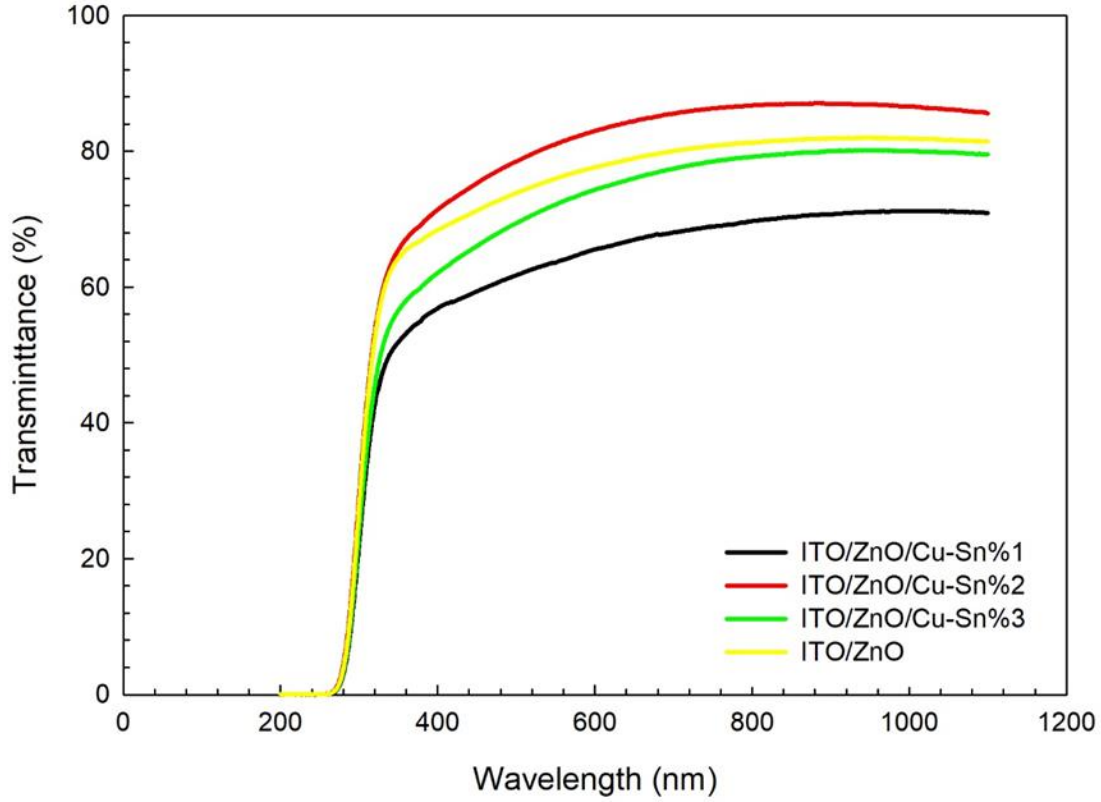

Figure 4.4 ITO/ZnO, ITO/ZnO/Sn 1%, ITO/ZnO/Sn 2%, ITO/ZnO/Sn 3% plotted using thin-film optical transmittance $(\alpha h\nu)^2(eVcm^{-1})^2$ measurements for energy conduction graphics

SEM morphology analysis was performed to better understand the morphology of the produced semiconductor thin film samples. The surface morphologies of undoped ZnO and ITO/ZnO/Sn 1%, ITO/ZnO/Sn 2%, ITO/ZnO/Sn 3% samples are given in Figure 4.5.

When the morphology of the undoped ZnO thin film sample was examined, it was observed that they grew together in clusters on the surface. It was observed that the surface morphology changed into spherical structures with Sn doped. As the Sn contribution ratio increased, it was observed that the structures tended to come together (Table 4.2).

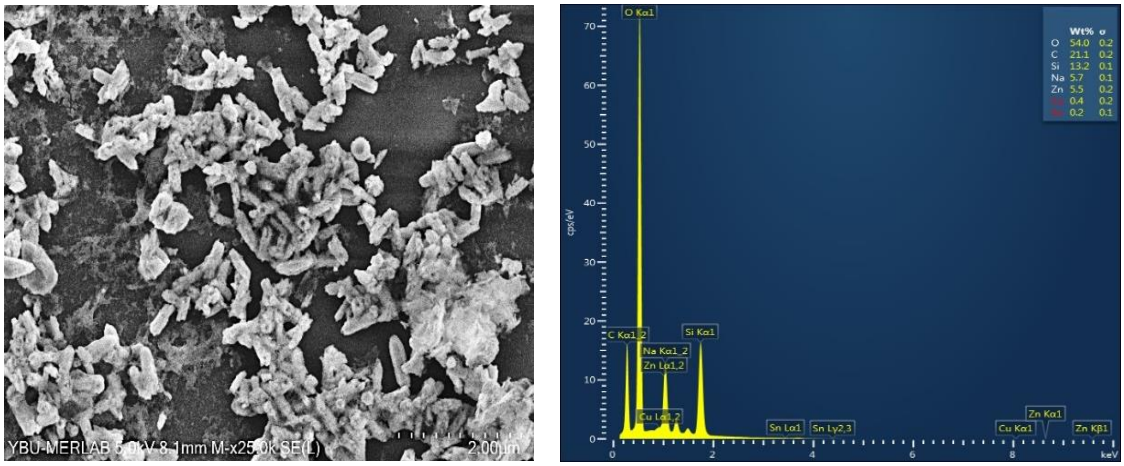

(a)

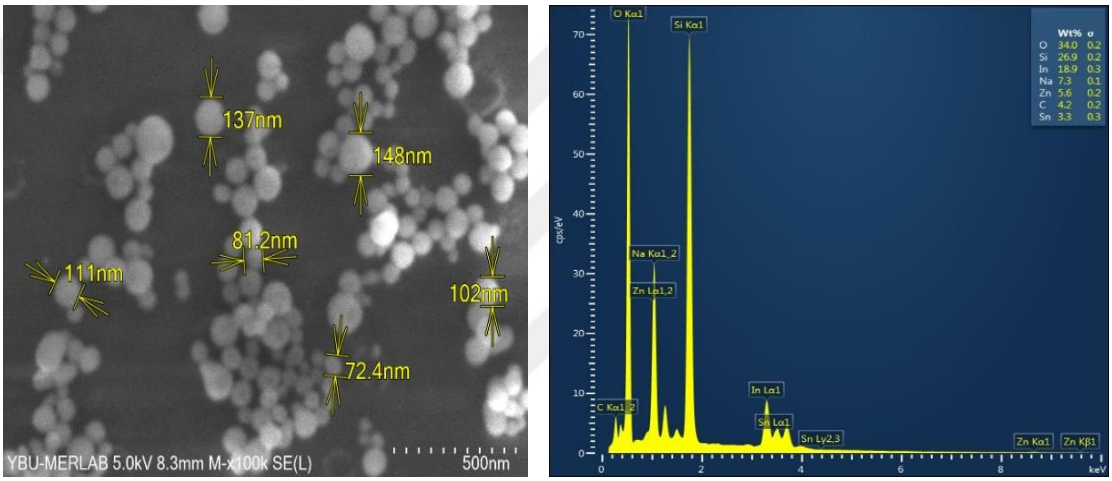

(b)

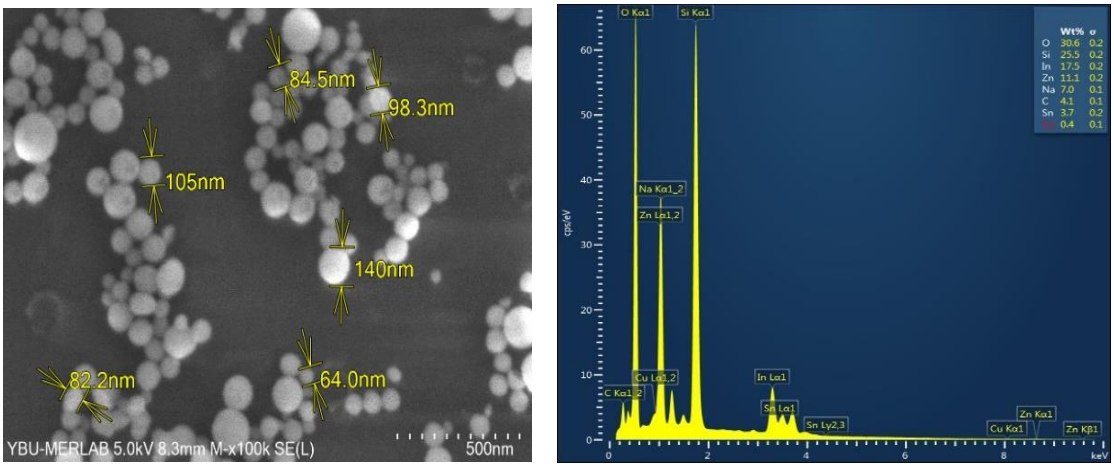

(c)

continued

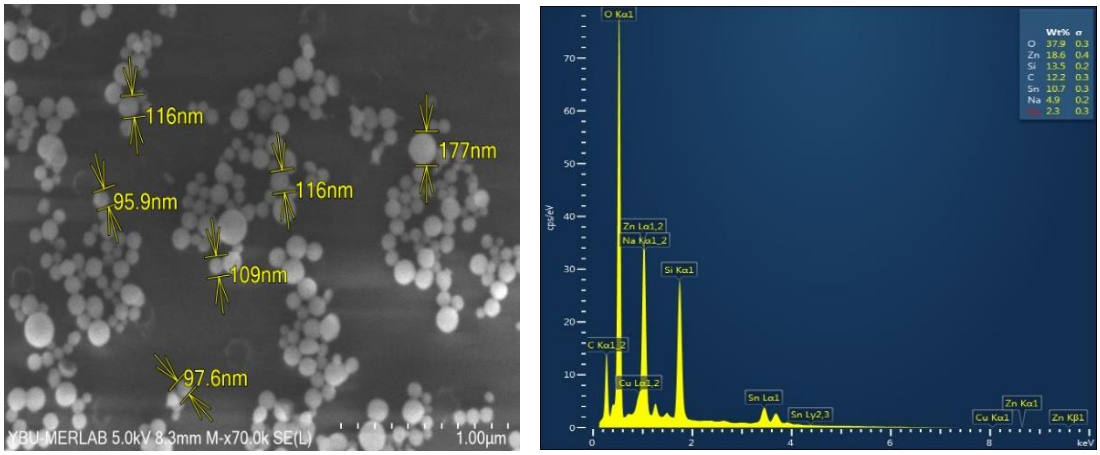

(d)

Figure 4.5 SEM analysis of thin films of (a) ITO/ZnO, (b) ITO/ZnO/Sn 1%, (c) ITO/ZnO/Sn 2%, (d) ITO/ZnO/Sn 3%

Table 4.2 Elemental parameters of thin films ITO/ZnO, ITO/ZnO/Sn 1%, ITO/ZnO/Sn 2%, ITO/ZnO/Sn 3% in EDS analysis

Sample Name	Zn Wt%	Si Wt%	O Wt%	C Wt%	Na Wt%	Cu Wt%	Sn Wt%	In Wt%
ITO/ZnO	5.5	13.2	54	3.1	5.7	0.4	0.2	-
ITO/ZnO/Sn 1%	5.6	26.9	34	4.2	7.3	-	3.3	18.9
ITO/ZnO/Sn 2%	11.2	25.5	30.6	4.1	7	0.4	3.7	17.5
ITO/ZnO/Sn 3%	18.6	13.5	37.9	12.2	4.9	2.3	10.7	-

4.5 X-Ray diffraction (XRD)

The results of X-ray diffraction (XRD) measurements of pure zinc oxide film (ZnO) doped with Cu and Sn in different proportions (1 %, 2 %, 3 %) prepared by SILAR method and of the form (a, b, c, d) showed that The X-ray diffraction curves for all prepared films are shown, and by analyzing these curves, the locations of the peaks, which appear sharply when beams of these rays are shed at different angles on the membrane, were dispersed, so that they can interfere constructively when the Bragg condition is available.

The dominant diffraction peaks are in the (110), (100) and (002) orientation, indicating the tetragonal crystal structure of SnO_2: F according to. It was observed that the peak intensities and slit widths of the films decreased as the Sn additive amount increased. In addition, as the doping ratio in the films increased, the peak intensities decreased and the slit-pipe widths increased compared to the undoped films ZnO (Figure 4.6).

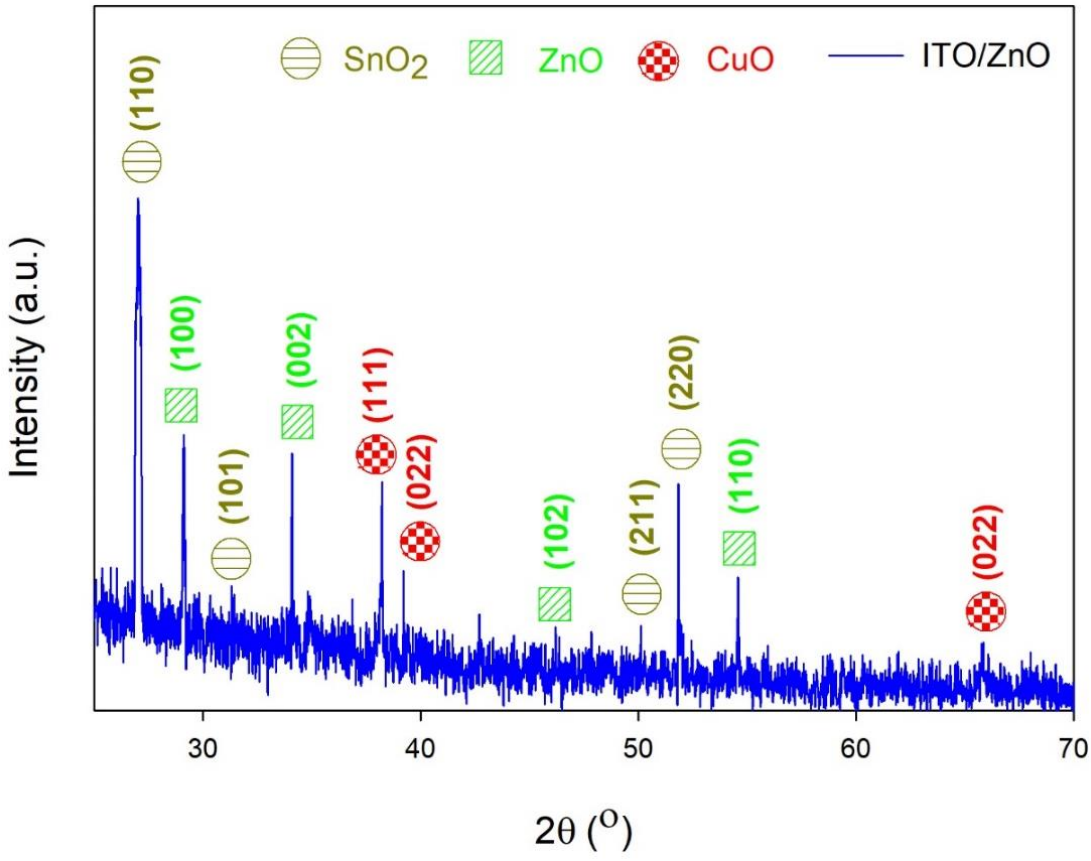

(a)

continued

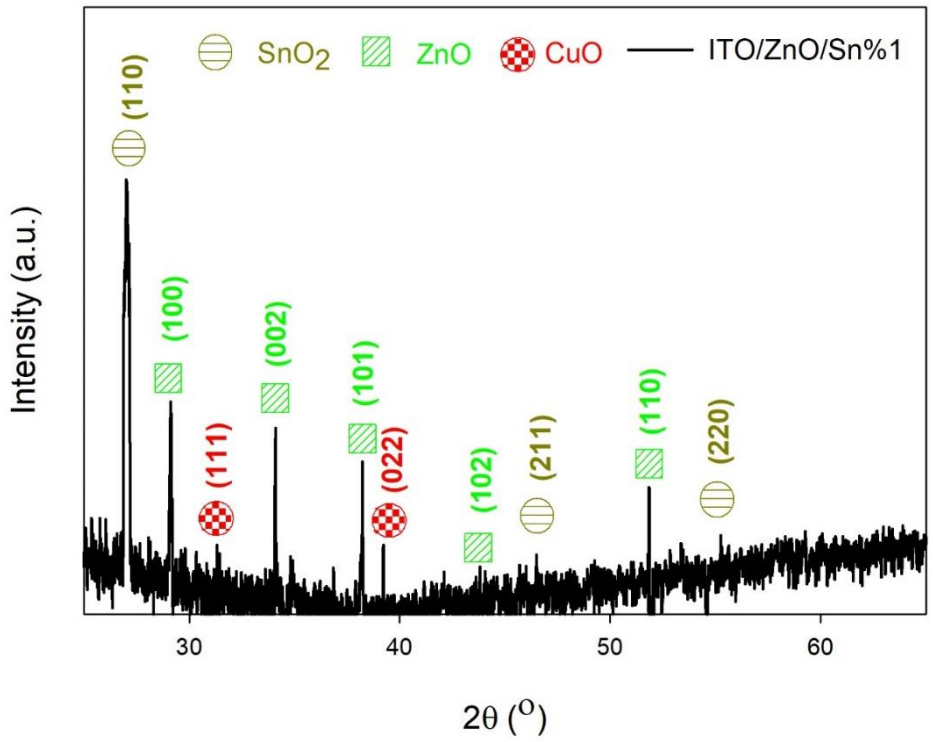

(b)

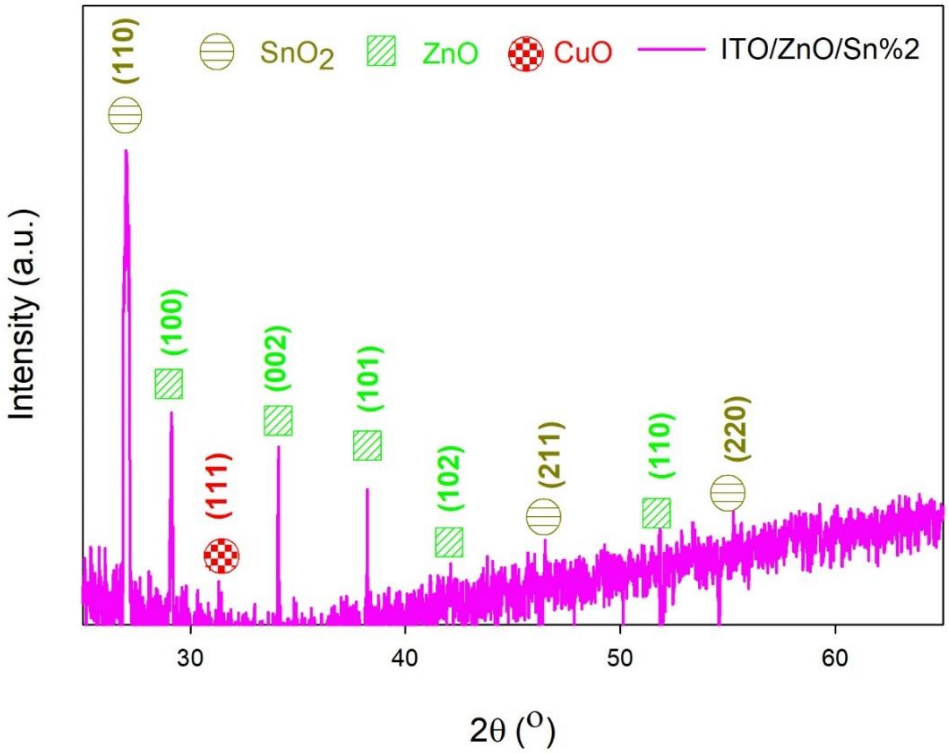

(c)

continued

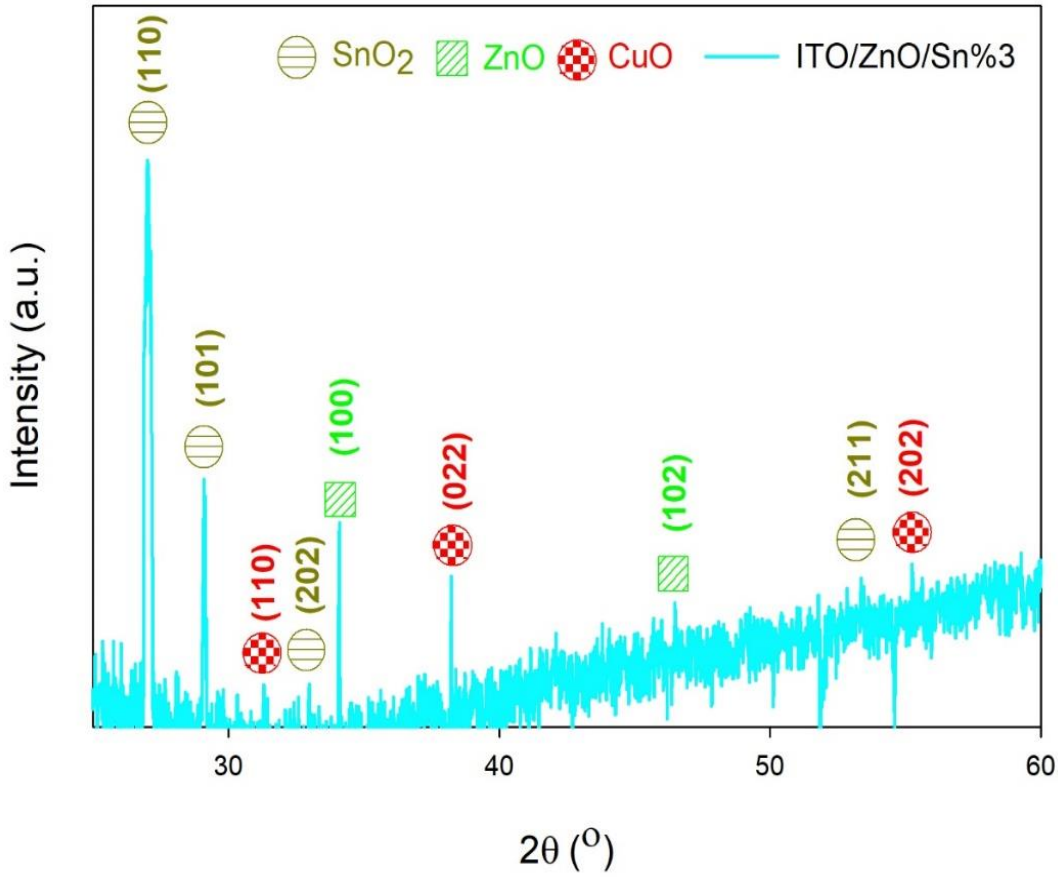

(d)

Figure 4.6 XRD analysis of thin films of (a) ITO/ZnO, (b) ITO/ZnO/Sn 1%, (c) ITO/ZnO/Sn 2%, (d) ITO/ZnO/Sn 3%

4.6 Electrical Conductivity Measurements

The characteristics of (Current-Voltage, C-V) are among the characteristics of the electrical conductivity mechanism, so the (current-voltage) relationship in the dark condition is an indicator of the resistance or resistivity and electrical conductivity of the thin films. Different doping ratios on these properties and determining the appropriate conditions to produce films with desirable specifications.

When studying the properties (Current - Voltage) in the dark and studying the effect of doping ratio on the electrical resistance of ZnO films, it was found that it shows a behavior closer to the behavior of metals, although it shows semi-conductive properties at times, as it behaves in a middle way between metals and semiconductors.

We have found that the process of doping with the conditions used in our research has positive results in the lack of electrical resistance of these membranes.

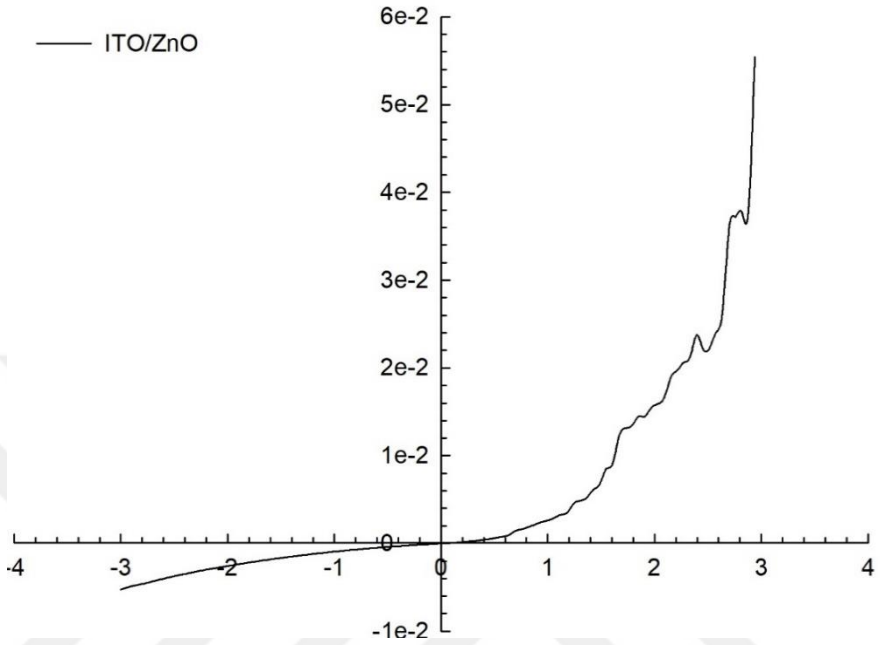

(a)

continued

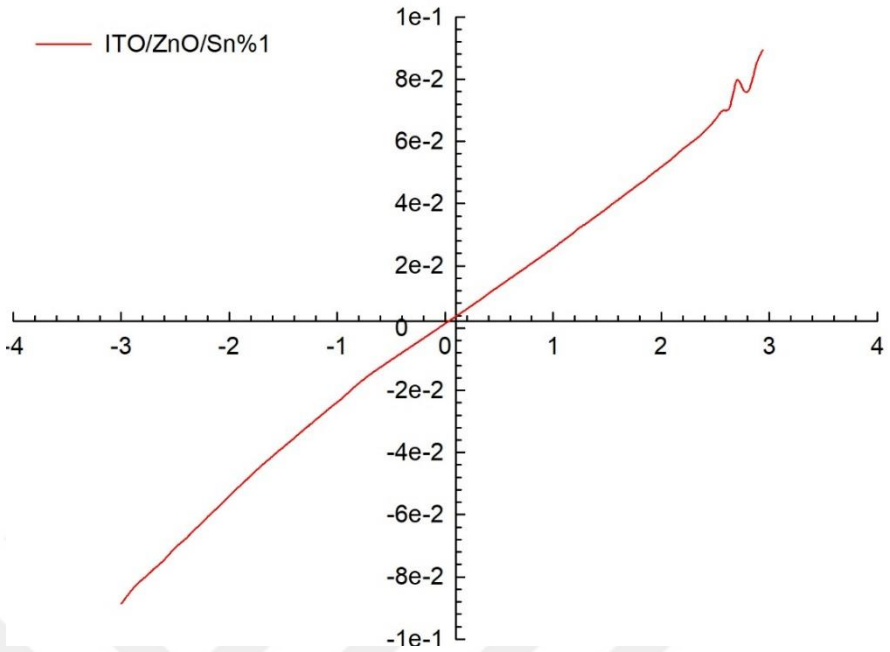

(b)

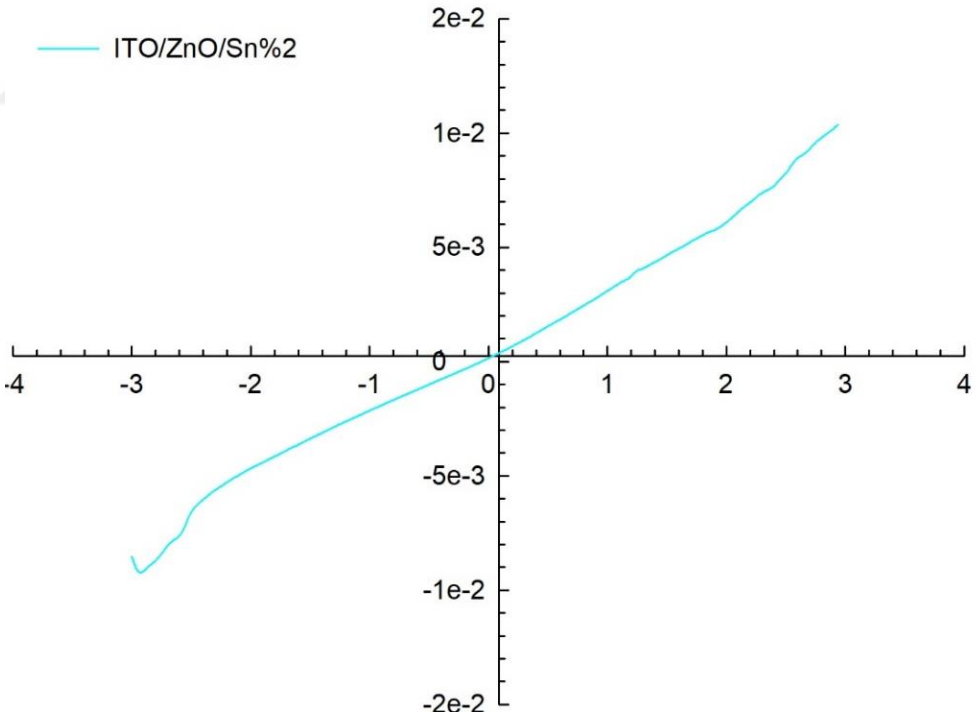

(c)

continued

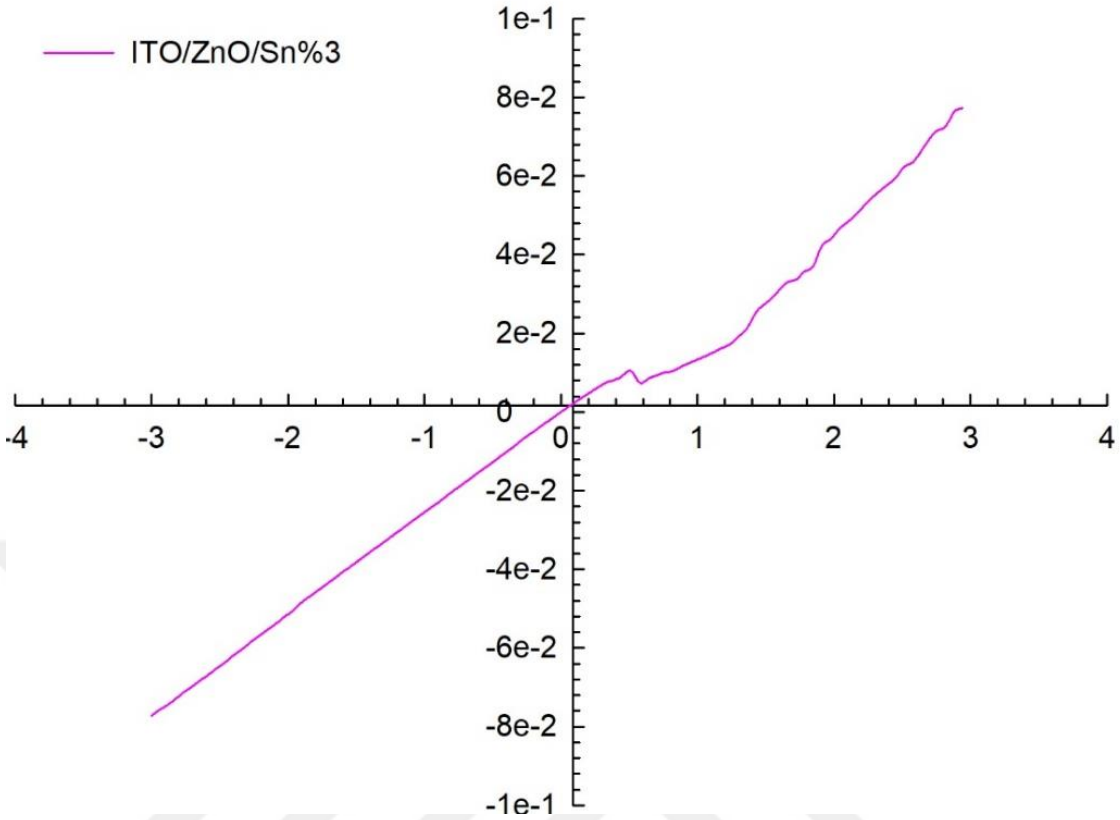

(d)

Figure 4.7 I-V plots of (a) ITO/ZnO, (b) ITO/ZnO/Sn 1%, (c) ITO/ZnO/Sn 2%, (d) ITO/ZnO/Sn 3% heterostructure

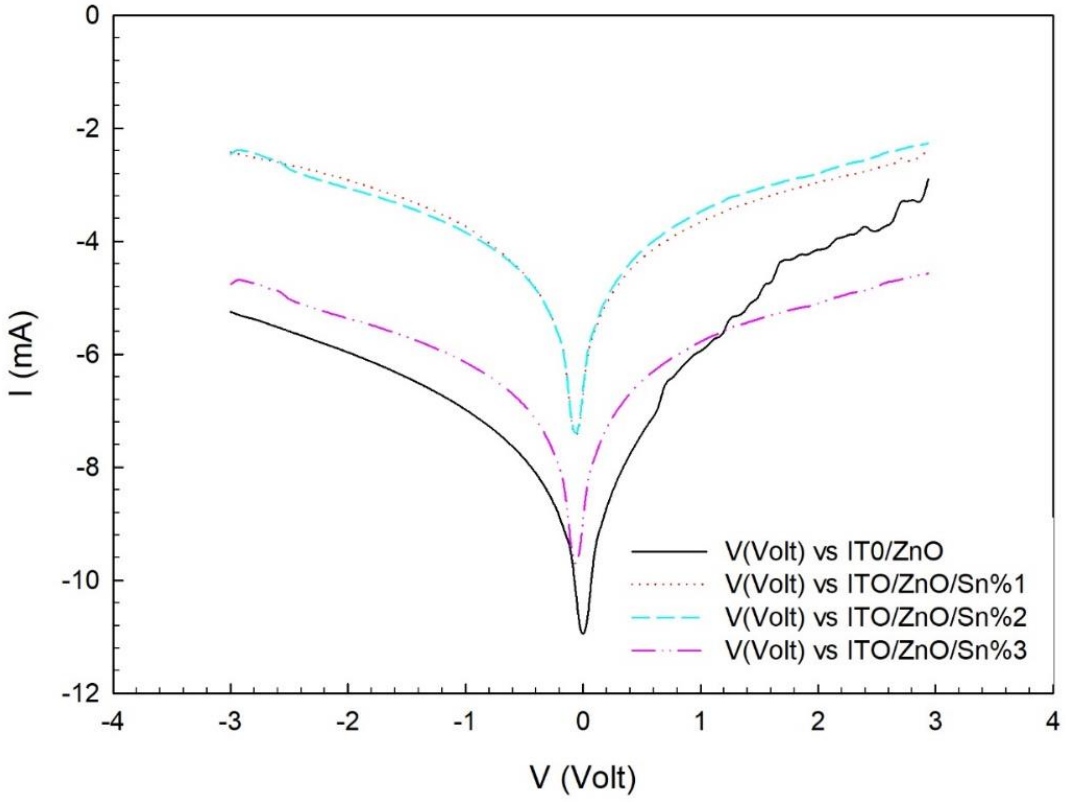

Figure 4.8 The log I-V plots of (a) ITO/ZnO, (b) ITO/ZnO/Sn 1%, (c) ITO/ZnO/Sn 2%, (d) ITO/ZnO/Sn 3% heterostructure

The I-V plots obtained in the dark and produced clear environment of the heterostructure are given in Figure 4.7. The log I-V plots of heterostructure are shown in Figure 4.8.

Table 4.3 The electrical parameters of (a) ITO/ZnO, (b) ITO/ZnO/Sn 1%, (c) ITO/ZnO/Sn 2%, (d) ITO/ZnO/Sn 3% heterostructure

Layer	**I_0 (A)**	**n**	**ϕ_B (eV)**
ITO/ZnO	6.01×10^{-8}	3.58	0.689
ITO/ZnO/Sn 1%	1.05×10^{-5}	3.69	0.725
ITO/ZnO/Sn 2%	1.38×10^{-6}	4.02	0.769
ITO/ZnO/Sn 3%	1.05×10^{-7}	2.45	0.742

$$Io=AA^{*}\mathbf{T^{2}}\ \mathbf{e}^{\left(-\frac{q\phi B}{kT}\right)} \quad (4.1)$$

where A is contact area, A* is Richardson constant, and ϕB is barrier height at zero bias Equation (4.1, 4.2).

$$n=\frac{q}{kT}\left(\frac{dV}{d(\ln (I)}\right) \quad (4.2)$$

barrier height was calculated with Equation (4.3).

$$\phi B=\frac{kT}{kq}\ln\left(\frac{AA*T^{2}}{Io}\right) \quad (4.3)$$

These calculated electrical parameters are given in Table 4.3. The lowest ITO/ZnO/Sn 3% layer contained the ideality factor, which was present in the largest ITO/ZnO layer. The reason for this is that as the thickness of the ZnO/Cu-Sn layer rises, the surface shape improves and the roughness values decrease. In terms of electrical characteristics, ITO/ZnO/Sn 3% was shown to be the best layer.

5. CONCLUSION AND RECOMMENDATIONS

Through the experimental and detailed study that we conducted on the formation of thin films in (ZnO) and by controlling many treatments that affect their structural, photometric and electrical properties such as coloration temperature, denaturation time, and the addition of impurities with different weight ratios.

The success of the SILAR technique in preparing ZnO thin films with high specifications similar to films prepared with more expensive and complex techniques. Obtaining homogeneous films with good optical properties.

Obtaining homogenous (spherical) nanometer granules with average diameters (64 nm - 148 nm), where it was noticed that the surface formation changed into spherical structures with (Sn) doped. Improvement of the optical and electrical properties of ZnO films upon co-doping (Sn- Cu).

The change in the energy gap (E_g) for zinc oxide films for certain doping ratios, as it reaches (3.42 eV) at the ratio 1 % of (Sn) and decreases to (3.35 eV) at the ratio 3 % of the impurity (Sn). The possibility of using zinc oxide films in solar cell applications due to their response in (I-V) measurements, as well as in gas and biological sensors due to their small diameters of about (70 nm).

Recommendations:

- Studying the effect of other numbers of zinc ions on the properties and structure of the formed membranes, such as: zinc chloride, zinc nitrate, etc.
- Studying the effect of other types of non-glass substrates such as silicone, aluminum, etc.
- Studying the effect of other types of impurities such as: (silver, aluminum, copper, etc.).

- Work to include these membranes in his system - solar cells and biological sensors.
- Studying the effect of etching factors on the shape and hardness of the formed granules, such as: triethanolamine, etc.

REFERENCES

Abdallah, B., Ismail, A., Kashoua, H., and Zetoun, W. 2018 Effects of deposition time on the morphology, structure, and optical properties of PbS thin films prepared by chemical bath deposition. Journal of Nanomaterials, 2018.

Al-Ani, S. K. (2008). Methods of determining the refractive index of thin solid films. Iraqi Journal of Applied Physics, 4: 17-23.

AL-Jawad, S. M. H., Sabr, A. S., and Elttayef, A. K. 2016. Doping Effect on Structure, Optical, and Sensing Properties of Nanocrystalline (SnO_2) Thin Films Prepared by Chemical Bath Deposition (CBD) Technique. Engineering and Technology Journal, 34(5 Part (B) Scientific).

Ayouchi, R., Martin, F., Leinen, D., and Ramos-Barrado, J. R. 2003. Growth of pure ZnO thin films prepared by chemical spray pyrolysis on silicon. Journal of Crystal Growth, 247(3-4): 497-504.

Bakr, N. A., Khodair, Z. T., and Saleh, A. M. 2018. Effect of Substrate Temperature on Structural and Optical Properties of ZnO Thin Films Prepared by APCVD Technique. International Journal of Applied Engineering Research, 13(12): 10796-10803.

Benhaoua, A., Rahal, A., Benhaoua, B., and Jlassi, M. 2014. Effect of fluorine doping on the structural, optical and electrical properties of SnO2 thin films prepared by spray ultrasonic. Superlattices and Microstructures, 70: 61-69.

Bernardi, M. I. B., Soledade, L. E., Santos, I. A., Leite, E. R., Longo, E., and Varela, J. A. 2002. Influence of the concentration of Sb_2O_3 and the viscosity of the precursor solution on the electrical and optical properties of SnO_2 thin films produced by the Pechini method. Thin Solid Films, 405(1-2): 228-233.

Biswal, R., Maldonado, A., Vega-Pérez, J., Acosta, D. R., and Olvera, M. D. L. L. 2014. Indium doped zinc oxide thin films deposited by ultrasonic chemical spray technique, starting from zinc acetylacetonate and indium chloride. Materials, 7(7): 5038-5046.

Burgelman, M. 2006. Cadmium telluride thin film solar cells: characterization, fabrication and modeling. Thin Film Solar Cells Fabrication, Characterization and Applications, 1: 277-324.

Chen, Z. C., Zhuge, L. J., Wu, X. M., and Meng, Y. D. 2007. Initial study on the structure and optical properties of Zn1-xFexO films. Thin Solid Films, 515(13): 5462-5465.

Choi, J. Y., Kim, K.-J., Yoo, J.-B., and Kim, D. 1998. Properties of cadmium sulfide thin films deposited by chemical bath deposition with ultrasonication. Solar Energy, 64(1-3): 41-47.

Gâlcă, A. C., Secu, M., Vlad, A., and Pedarnig, J. D. 2010. Optical properties of zinc oxide thin films doped with aluminum and lithium. Thin Solid Films, 518(16): 4603-4606.

Goriunova, N. A., and Anderson, J. C. 1965. The chemistry of diamond-like semiconductors. Chapman and Hall London. 12-26.

Hafdallah, A. 2007. Étude du dopage des couches minces de ZnO élaborées par spray ultrasonique.

He, R., Tang, B., Ton-That, C., Phillips, M., and Tsuzuki, T. 2013. Physical structure and optical properties of Co-doped ZnO nanoparticles prepared by co-precipitation. Journal of Nanoparticle Research, 15(11): 1-8.

Hussein, S. A., Hmeed, A., and Hadi, A. S. 2017. Study of the Structural and Optical Properties of.. Thin Films Copper Sulfide (CuS) Prepared by Chemical Spray Pyrolysis.

Kamal, H., Elmaghraby, E. K., Ali, S. A., and Abdel-Hady, K. 2004. Characterization of nickel oxide films deposited at different substrate temperatures using spray pyrolysis. Journal of Crystal Growth, 262(1-4): 424-434.

Kang, K.-M., Wang, Y., Kim, M., and Park, H.-H. 2018. Study on properties of Ga/F-co-doped ZnO thin films prepared using atomic layer deposition. Thin Solid Films, 660: 913-919.

Khan, Z. R., Khan, M. S., Zulfequar, M., and Khan, M. S. 2011. Optical and structural properties of ZnO thin films fabricated by sol-gel method. Materials Sciences and Applications, 2(5): 340-345.

Khoudro, A., and Najeeb, S. H. 2020. Studying the Infrared Spectroscopy of the SnO_2: Sb (x = 0.00, 0.01) Powders.

Kim, K. T., Kim, G. H., Woo, J. C., and Kim, C. I. 2008:. Characteristics of Nickel-doped Zinc Oxide thin films prepared by sol-gel method. Surface and Coatings Technology, 202(22-23): 5650-5653.

Kumar, P., Kumar, A., Dixit, P. N., and Sharma, T. P. 2006. Optical, structural and electrical properties of zinc sulphide vacuum evaporated thin film. Indian Journal of Pure and Applied Physics, 44(9): 690-693.

Lee, D. N. 2003. Elastic properties of thin films of cubic system. Thin Solid Films, 434(1-2): 183-189.

Mabayoje, O., Shoola, A., Wygant, B. R., and Mullins, C. B. 2016. The role of anions in metal chalcogenide oxygen evolution catalysis: electrodeposited thin films of nickel sulfide as "pre-catalysts." ACS Energy Letters, 1(1): 195-201.

Mazhir, S. N., and Harb, N. H. 2015. Influence of concentration on the structural, optical and electrical properties of TiO_2: CuO thin film Fabricate by PLD. IOSR Journal of Applied Physics, 7(6): 14-21.

Mosiori, C. O. 2015. Inorganic Ternary Thin Films: Anaysis of Optical Properties. Anchor Academic Publishing (aap_verlag).

Moustaghfir, A. 2004. Élaboration et caractérisation de couches minces d'oxyde de zinc. Application à la photoprotection du polycarbonate. Université Blaise Pascal-Clermont-Ferrand II.

Pal, J., and Chauhan, P. 2009. Structural and optical characterization of tin dioxide nanoparticles prepared by a surfactant mediated method. Materials Characterization, 60(12): 1512-1516.

Pandya, S., and Raval, K. 2017. Investigation of structural, morphological and optical properties of cadmium sulphide (CdS) thin films at different Cd/S concentration deposited by chemical technique. Journal of Materials Science: Materials in Electronics, 28(23): 18031-18039.

Pathan, H. M., and Lokhande, C. D. 2004. Deposition of metal chalcogenide thin films by successive ionic layer adsorption and reaction (SILAR) method. Bulletin of Materials Science, 27(2): 85-111.

Perna, G., and Capozzi, V. 2002. Analysis of optical spectra of CdS and CdSe films deposited on a sapphire substrate by laser ablation technique. The European Physical Journal B-Condensed Matter and Complex Systems, 26(4): 401-406.

Rahal, A. (2013). Elaboration des verres conducteurs par déposition de ZnO sur des verres ordinaires. UNIVERSITE D'ELOUED.

Ratheesh Kumar, P. M., Vijayakumar, K. P., and Sudha Kartha, C. 2007. On the origin

of blue-green luminescence in spray pyrolysed ZnO thin films. Journal of Materials Science, 42(8): 2598-2602.

Reddy, K. T. R., Reddy, T. B. S., Forbes, I., and Miles, R. W. 2002. Highly oriented and conducting ZnO: Ga layers grown by chemical spray pyrolysis. Surface and Coatings Technology, 151: 110-113.

Richard, B. D. 2013. Thermal Infrared Reflective Metal Oxide Sol-Gel Coatings for Carbon Fiber Reinforced Composite Structures.

Saha, B., Das, S., and Chattopadhyay, K. K. 2007. Electrical and optical properties of Al doped cadmium oxide thin films deposited by radio frequency magnetron sputtering. Solar Energy Materials and Solar Cells, 91(18): 1692-1697.

Srivastava, S., Haridas, M., and Basu, J. K. 2008. Optical properties of polymer nanocomposites. Bulletin of Materials Science, 31(3): 213217.

Subramanyam, T. K., Srinivasulu Naidu, B., and Uthanna, S. 2000. Physical properties of zinc oxide films prepared by dc reactive magnetron sputtering at different sputtering pressures. Crystal Research and Technology: Journal of Experimental and Industrial Crystallography, 35(10): 1193-1202.

Tabet, A. 2013. Optimisation des conditions d'élaboration (température de substrat et distance bec-sub strat) des films minces de ZnO par spray .

Turgut, G., Sonmez, E., and Duman, S. 2015. Determination of certain sol-gel growth parameters of nickel oxide films. Ceramics International, 41(2): 2976-2989.

Van Hieu, N., Duc, N. A. P., Trung, T., Tuan, M. A., and Chien, N. D. 2010. Gas-sensing properties of tin oxide doped with metal oxides and carbon nanotubes: A competitive sensor for ethanol and liquid petroleum gas. Sensors and Actuators B: Chemical, 144(2): 450-456.

Wang, M. C., Lin, H. J., and Yang, T. S. 2009. Characteristics and optical properties of iron ion (Fe3+)-doped titanium oxide thin films prepared by a sol–gel spin coating. Journal of Alloys and Compounds, 473(1-2): 394-400.

Yadav, A. A., Masumdar, E. U., Moholkar, A. V, Neumann-Spallart, M., Rajpure, K. Y., and Bhosale, C. H. 2009. Electrical, structural and optical properties of SnO_2: F thin films: Effect of the substrate temperature. Journal of Alloys and Compounds, 488(1): 350-355.

Yi, G., Wu, Z., and Sayer, M. 1988. Preparation of Pb (Zr, Ti) O_3 thin films by sol gel

processing: Electrical, optical, and electro-optic properties. Journal of Applied Physics, 64(5): 2717-2724.

Ynineb, F. 2015. Etude et realisation de structures a base d'oxyde de Zinc.

Zhang, H., Lu, S., Xu, W., and Yuan, F. 2013. First-principles study of electronic structures and photocatalytic activity of low-Miller-index surfaces of ZnO. Journal of Applied Physics, 113(3): 34903.

Zhou, W., Apkarian, R., Wang, Z. L., and Joy, D. 2006. Fundamentals of scanning electron microscopy (SEM). In Scanning microscopy for nanotechnology (pp. 1-40). Springer.